TABLE 1. Expression of growth factor and growth factor receptor genes in mesenchymal stem cells

		H4-I			UE6E7T-12			UE7T-13		
Probe set	Description	NV	Flag	Raw	NV	Flag	Raw	NV	Flag	Raw
Growth factor receptor										
201983_s_at	Epidermal growth factor receptor	1.08	P	2172	1.18	P	3113	0.47	P	2079
202273_at	Platelet-derived growth factor receptor, beta	3.33	P	4049	2.03	P	3252	0.79	P	2076
203131_at	Platelet-derived growth factor receptor, alpha	1.07	P	4990	1.19	P	7328	0.52	P	5256
203627_at	Insulin-like growth factor	2.07	P	1437	1.03	P	938	0.97	P	1467
205051_s_at	v-kit sarcoma viral oncogene	1.73	A	123	0.66	A	62	2.46	A	380
205876_at	Transforming growth factor receptor	1.03	P	2749	0.66	P	2339	0.48	P	2785
20858_at	Nerve growth factor receptor	1.32	A	19	1.07	A	20	2.19	A	68
208944_at	Met proto-oncogene	0.80	P	1333	1.00	P	2206	0.38	P	1376
210316_at	Leukemia inhibitory factor receptor	1.00	P	114	1.60	P	239	0.80	M	197
211535_s_at	Fibroblast growth factor receptor	1.31	P	3126	0.89	P	2803	0.35	P	1818
Growth factor										
203085_s_at	Transforming growth factor, beta	0.49	P	1134	1.00	P	3055	0.38	P	1904
204421_s_at	Fibroblast growth factor 2	2.12	P	3955	1.00	P	2454	0.43	P	1719
205016_at	Transforming growth factor, alpha	7.66	P	522	0.43	A	38	0.88	A	131
205266_at	Leukemia inhibitory factor	7.15	P	5039	0.49	P	456	0.46	A	710
205463_s_at	Platelet-derived growth factor, alpha	1.07	P	750	1.00	P	924	0.72	A	1112
206254_at	Epidermal growth factor	0.41	A	21	1.59	A	106	0.63	A	70
206414_at	Nerve growth factor	2.76	P	1865	0.81	P	722	1.00	P	1467
209540_at	Insulin-like growth factor 1	1.61	A	24	0.47	A	9	6.97	A	223
209960_at	Hepatocyte growth factor	0.79	A	87	1.07	P	156	0.96	A	230
210512_s_at	Vascular endothelial growth factor	2.09	P	7536	0.40	P	1913	0.23	P	1819
211124_s_at	Kit ligand	0.31	A	89	1.95	P	739	1.23	P	703
216055_at	Platelet-derived growth factor, beta	1.00	A	63	1.42	A	118	2.16	A	296

NV, normalized value; P, presence; A, absence; M, marginal.

phosphoethanolamine, 10 ng/ml PDGF-BB, and 10 ng/ml bFGF). We then investigated the effect of the LS medium on primary cultures of marrow-derived mesenchymal cells (Fig. 1B), cartilage-derived chondrocytes (Fig. 1C), and fat tissue-derived preadipocytes (Fig. 1D). All cell types tested grew at least 100-fold more rapidly in the combined growth medium than in DMEM supplemented with 10% serum during 3 weeks after the start of cultivation.

Cell life span and p16ink4a expression in the LS medium

In light of the fact that chemically defined growth medium containing growth factor(s) induces premature growth arrest of foreskin fibroblasts (Ramirez et al., 2001), we investigated the life span and p16ink4a induction of MF cells cultivated in LS growth medium (Fig. 2A–C). The cells proliferated more rapidly in the LS growth medium than in the conventional medium. However, the cells cultured in the LS growth medium stopped growing and entered senescence or the growth arrest stage after fewer population doublings (Fig. 2A). MF cells with the broad and flat cytoplasm exhibited high SA-β-galactosidase activity (Fig. 2B). p16ink4a, which induces premature senescence and is a marker for cell stress, was induced after fewer PDs in the LS growth medium than in the conventional medium (Fig. 2C).

Reversibility of the induction of p16ink4a expression by the culture conditions

We tested whether p16ink4a was induced during cellular aging or increased population doubling or was induced by unidentified molecule(s) in the LS medium (Fig. 2D,E). The MF cells grown in the conventional medium or the LS medium were passaged into two dishes; one was maintained in the same growth medium and the other was cultured in a different growth medium for analysis of p16ink4a expression. The expression level of p16ink4a gradually increased as the passage number of the cells increased in the LS medium (Fig. 2D, lanes 8–10), but the expression level of p16ink4a in the cells cultured in the conventional medium remained very low or was rather decreased (Fig. 2D, lanes 1–3), implying that the induction of p16ink4a protein depended on cell cultivation in the LS medium. Surprisingly, the high-level p16ink4a expression returned to an undetectable level when the cells were switched to culturing in the conventional medium after culturing in the LS growth medium (Fig. 2D, lanes 11–14) and vice versa: p16ink4a started to be expressed when the growth medium was changed from the conventional medium to the LS growth medium (Fig. 2D, lanes 4–7), suggesting that the p16ink4a expression depended on the culture medium and was completely reversible.

Identification of molecule(s) responsible for p16ink4a expression in the LS medium

To identify molecule(s) in the LS medium responsible for the expression of p16ink4a, we removed individual supplements to test their influence on the expression of p16ink4a protein (Fig. 3A, Suppl. Fig. 2). The p16ink4a protein level was significantly decreased by removing PDGF-BB or bFGF from the LS medium, and was decreased to an undetectable level by removing both PDGF-BB and bFGF from the LS medium; however, the medium without these growth factors did not support cell growth sufficiently. Interestingly, the addition of 10% FCS restored the cell growth but did not up-regulate p16ink4a (Fig. 3B, lanes 1 and 4). We also added PDGF-BB and bFGF at different concentrations to the LS medium without any other growth factors and found that the induction of p16ink4a protein level depended on the concentration of both PDGF-BB and bFGF (Fig. 3B, lanes 4–6). These results demonstrate that both PDGF-BB and bFGF are key factors for the induction of p16ink4a protein expression in mesenchymal stem cells. The expression level of p16ink4a was also increased in a concentration-dependent manner when the cells were cultured in the conventional medium supplemented with both PDGF and bFGF (Fig. 3B, lanes 7–9).

Since cells become more sensitive to culture stress in serum-free or low-serum medium, we cultured the cells in different concentrations of serum or oxygen to see if low serum and/or oxygen stress induced p16ink4a expression in LS medium (Fig. 3C, D) (Chen et al., 1995; Itahana et al., 2003; Parrinello et al., 2003). Serum or oxygen concentration did not affect the p16ink4a level at all, implying that low serum and

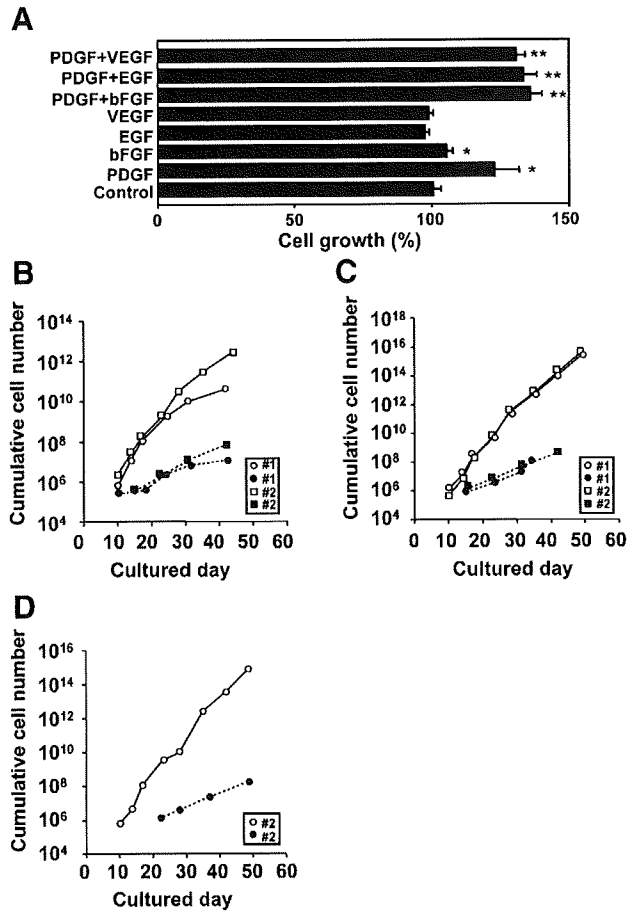

Fig. 1. Accelerated growth of mesenchymal cells in the growth medium supplemented with growth factors. A: The mean ± SD from triplicate determinations in cell growth. Growth rate of MF cells in response to VEGF (10 ng/ml), EGF (10 ng/ml), bFGF (10 ng/ml), and PDGF (10 ng/ml) in culture medium supplemented with 0.5% FCS. Absorbance (450 nm) in the WST-1 assay was measured as an indicator of cell growth 4 days after the addition of growth factors. The cell growth in the same culture conditions without growth factors was regarded as equal to 100%. The statistically analysis was performed by ANOVA and Fisher's t-test. $^{*}P < 0.05$; $^{**}P < 0.005$. B–D: Growth of marrow-derived mesenchymal cells (B), cartilage-derived chondrocytes (C) and fat tissue-derived preadipocytes (D) in primary culture in the combined growth medium (open circles and open squares) and DMEM supplemented with 10% FCS (closed circles and closed squares). The culture conditions, that is, the combined growth medium (LS growth medium), are described in detail in Cells and Cell Culture Section. The surgical specimens from irreversibly de-identified donors are numbered #1 and #2.

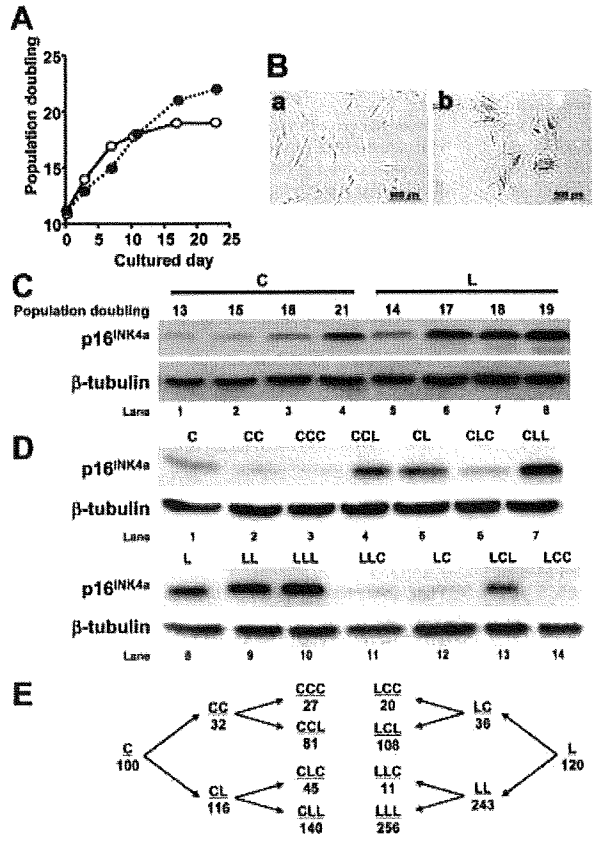

Fig. 2. In vitro growth of marrow-derived MF cells and time course analysis of p16ink4a protein levels. A: The population doublings of MF cells at 10 PDs cultured in the LS growth medium (open circles) and conventional medium (closed circles) are shown (see Cells and Cell Culture Section). Cell proliferative capacity was assessed by calculating the total number of population doublings (population doubling level or accumulative population doublings), using the formula $\log_{10}$ (total number of cells/starting number of cells)/$\log_{10}2$. The number of cells was counted by ViCell (Beckman Coulter) at each passage. The cells proliferated more rapidly in the LS growth medium than in the conventional medium. However, the cells cultured in the LS growth medium stopped growing and entered senescence or the growth arrest stage after fewer population doublings. B: SA-β-galactosidase activity of MF cells. a: No SA-β- galactosidase activity in the growth phase at PD 10. b: MF cells became broad and flat, ceased to proliferate, and exhibited high SA-β-galactosidase activity as indicated by their cytoplasm staining blue at PD 19. C: p16ink4a, a marker for cell stresses such as oxidative substances, ultraviolet light, and osmotic pressure, in MF cells was analyzed by Western blotting. Cells cultured for the periods indicated in the LS growth medium (L) and conventional medium (C) were assayed. Expression of β-tubulin protein was monitored as a loading control. D: p16ink4a in MF cells cultured in the sequential combinations indicated of LS growth medium (L) and conventional medium (C) were assayed. Expression of β-tubulin protein was monitored as a loading control. The cells were cultured until reaching semiconfluence in the growth medium indicated (L or C) and examined for p16ink4a expression by Western blot analysis. The cells proliferated more rapidly in the LS growth medium than in the conventional medium. The cells at semiconfluence in each culture condition were passaged and cultured in the growth medium indicated (CC, CL, LC, or LL), and were assayed for p16ink4a expression: for example, "LC" indicates that the cells were cultured until semiconfluence in the LS growth medium and then cultured in the conventional growth medium after passage. The cells were again passaged from each condition and cultured in the growth medium indicated, and were assayed for p16ink4a. E: Quantification of p16ink4a expression level. The numbers shown were obtained from the results of Western blot analysis (part D). p16ink4a level in MF cells in the conventional medium (lane 1 of part D) were regarded as equal to 100. [Color figure can be viewed in the online issue, which is available at www.interscience.wiley.com.]

oxygen concentration were not responsible for the up-regulation of p16ink4a.

Involvement of PDGF-BB and PDGF receptor β-chain (PDGFRβ) in induction of p16ink4a protein

We performed flow cytometric analysis to investigate which growth factor receptor(s) were expressed (Fig. 4). The analysis clearly revealed that MF cells were positive for CD140b, a PDGFRβ, and negative for CD140a, a PDGFR α-chain (PDGFRα) (Fig. 4A). PDGF is a dimer of two possible subunit proteins, A-chain and B-chain; PDGF A-chain binds to PDGFRα, while PDGF B-chain binds to either PDGFRα or PDGFRβ (Fig. 4B) (Seifert et al., 1993). We then investigated the signaling

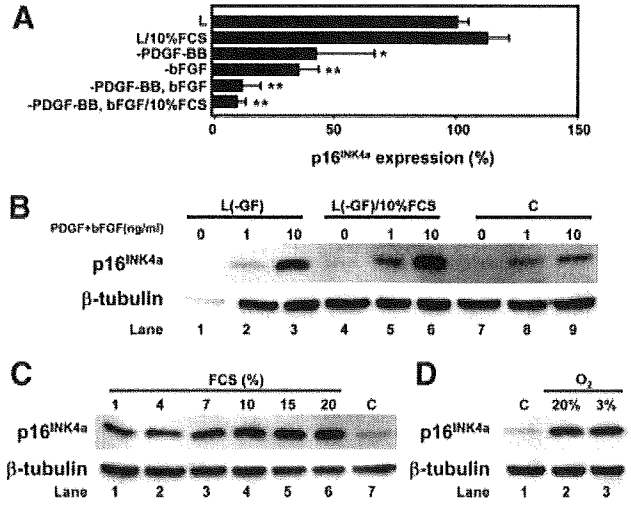

Fig. 3. Effect of PDGF-BB and bFGF on p16ink4a expression in MF cells. A: MF cells were cultured for 7 days in LS medium (L), LS growth medium supplemented with 10% FCS (L/10%FCS), without PDGF-BB (-PDGF-BB), without bFGF (-bFGF), without PDGF-BB and bFGF (-PDGF, bFGF), without PDGF-BB and bFGF, and supplemented with 10% FCS (-PDGF, bFGF/10%FCS). Equal amounts of protein extracts were separated by SDS–PAGE and analyzed by Western blotting with anti-p16ink4a and anti-β-tubulin antibodies. p16ink4a/β-tubulin expression of MF cells in LS medium (L) was regarded as equal to 100%. The mean ± SD is calculated from triplicates of band densities as determined by Image J 1.38x (NIH, USA). The statistic analysis was performed by ANOVA and Fisher' s t-test. *$P < 0.05$; **$P < 0.005$. B: MF cells were cultured for 7 days in growth factor-free LS medium (L(-GF)), growth factor-free LS medium supplemented with 10% FCS (L(-GF)/10% FCS), or the conventional medium (C), supplemented with the indicated concentration of both PDGF-BB and bFGF. C: The effect of the serum concentration in LS medium on the p16ink4a expression level. The MF cells were cultured for 7 days in LS medium supplemented with the indicated concentration of FCS (lanes 1–6). Culturing in the conventional medium (C) served a as a control (lane 7). D: Effect of oxygen concentration on the p16ink4a expression. The MF cells were cultured for 7 days in the LS medium at 20% oxygen (lane 2) or 3% oxygen (lane 3). Culturing in the conventional medium (C) at 20% oxygen served as a control (lane 1).

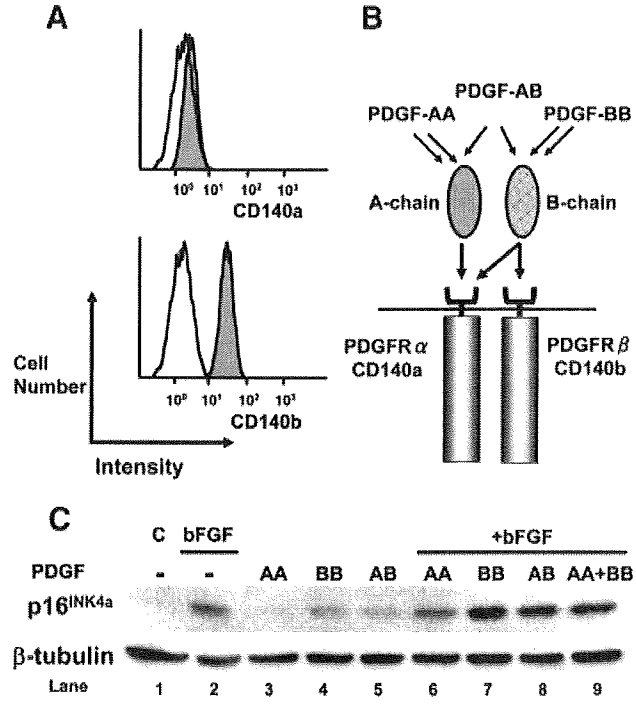

Fig. 4. Expression of p16ink4a protein by PDGF B-chain. A: Flow cytometric analysis using antibodies to CD140a and CD140b in MF cells. B: PDGF A-chain binds to PDGFRα and PDGF B-chain binds to either PDGFRα or PDGFRβ. The two PDGF receptor subunits can form three types of PDGF receptors, and PDGF-BB can bind to all three forms of the receptor. C: MF cells were cultured for 7 days in LS medium supplemented with lane 1: no growth factor; lane 2: bFGF; lane 3: PDGF-AA; lane 4: PDGF-BB; lane 5: PDGF-AB; lane 6: PDGF-AA and bFGF; lane 7: PDGF-BB and bFGF; lane 8: PDGF-AB and bFGF; or lane 9: PDGF-AA, PDGF-BB and bFGF. The concentrations of PDGF-AA, PDGF-AB, PDGF-BB, and bFGF were 30 ng/ml, 30 ng/ml, 30 ng/ml, and 10 ng/ml, respectively. Equal amounts of protein extracts were separated by SDS–PAGE and analyzed by Western blotting with anti-p16ink4a (upper column) and anti-β-tubulin (lower column) antibodies.

effects of all three isoforms (PDGF-AA, PDGF-AB, and PDGF-BB) for p16ink4a protein expression. The protein level of p16ink4a was induced when MF cells were cultured with PDGF-BB and PDGF-AB (Fig. 4C). PDGF-AA did not induce p16ink4a, consistent with the results obtained from the FACS analysis. These results suggest that PDGF B-chain induced p16ink4a protein through binding to its receptor, PDGF receptor β-chain, in MF cells. bFGF exhibited a synergistic effect with PDGF-BB for the level of p16ink4a induction (Fig. 4C).

The effects of growth factors on the expression of p16ink4a and on cell growth in the marrow-derived mesenchymal stem cells

To determine the relationship between p16ink4a induction and cell growth, we investigated the expression level of p16ink4a protein in MF cells exposed to different combinations of various growth factors, that is, aFGF, bFGF, EGF, VEGF, and PDGF-BB (Schichor et al., 2006; Tamama et al., 2006; Ng et al., 2008) (Fig. 5A). Among them, PDGF-BB and bFGF significantly induced p16ink4a protein. We then examined cell growth in cultures treated with combinations of the growth factors (Fig. 5B). A positive correlation ($R = 0.7$) was observed between the p16ink4a expression and cell growth in the MF cells exposed to growth factors (Fig. 5C). Since the p16ink4a expression is known to be mediated by mitogen-activated protein (MAP) kinases and blocked by their inhibitors (Lin et al., 1998; Wang et al., 2002; Iwasa et al., 2003), we tested whether p16ink4a was downregulated by PD98059, a specific inhibitor of MEK1 (Bébien et al., 2003; Williamson et al., 2004; Shimo et al., 2007), and by SB203580, a specific inhibitor of p38 MAPK (Bébien et al., 2003; Williamson et al., 2004; Shimo et al., 2007). Expression of p16ink4a was inhibited by both PD98059 and SB203580 (Fig. 5D), indicating that the induction of p16ink4a protein by growth factor stimulation is mediated via the ERK/p38 MAPK signal pathway.

Discussion

Establishment of minimal conditions for mesenchymal stem cells

Most animal cells can live, multiply, and even express differentiated properties under appropriate surroundings in tissue-culture dishes (Alberts, 2002). Primary cells dissociated from tissues were cultured and analyzed biochemically the effects of adding or removing specific molecules, such as hormones or growth factors. Cell culture conditions vary in a cell-specific manner and cells can therefore be categorized or defined by their requirements. Mesenchymal cell biology is a

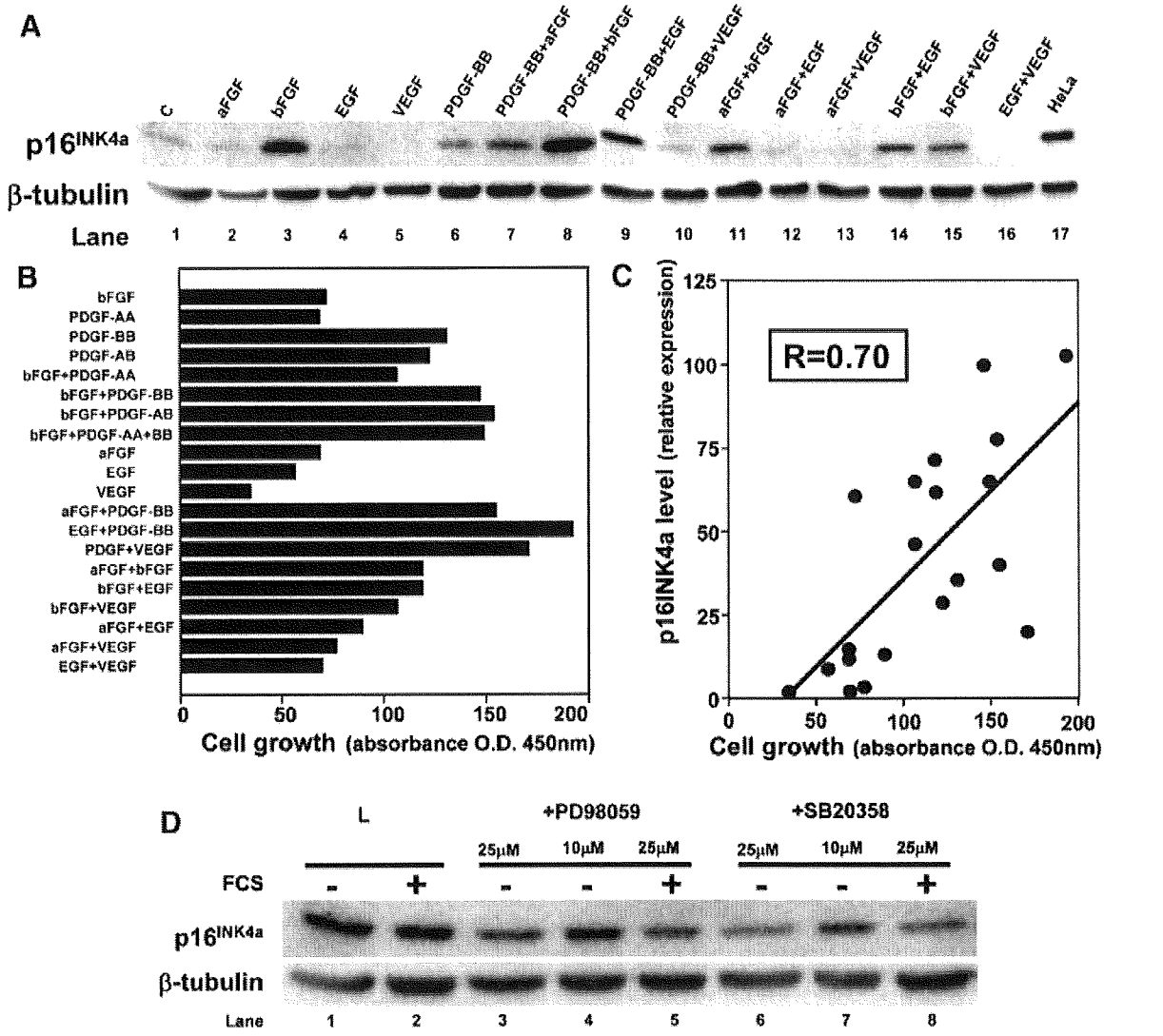

Fig. 5. The effects of various growth factors on the expression of p16ink4a and the cell growth of marrow-derived MF cells. A: MF cells were cultured in growth factor-free LS medium with the indicated growth factors for 7 days. B: MF cells were cultured in LS medium with the indicated growth factors for 7 days after growth factor starvation for 24 hr. Cell number was estimated by the WST-1 colorimetric assay. The x-axis shows the values of absorbance (450 nm) as an indicator of cell number. C: The correlation between the cell growth determined by the WST-1 colorimetric assay and the expression level of p16ink4a protein. The correlation factor (R) equals 0.7. D: The effect of MAPK inhibitors in LS medium on the p16ink4a expression of MF cells. The MF cells were cultured for 7 days in LS medium (lanes 1–2: L) supplemented with the indicated concentration of PD98059 (lanes 3–5) or SB20358 (lanes 6–8). To maintain cell viability, FCS was added to a final concentration of 10% (lanes 5 and 8). Culturing in the conventional medium without (lane 1) or with additional FCS (lane 2: Final FCS concentration was 10%) served as a control. Equal amounts of protein extracts were separated by SDS–PAGE and analyzed by Western blotting with anti-p16ink4a (upper column) and anti-β-tubulin (lower column D) antibodies.

complex, rapidly evolving field (Toyoda et al., 2007). Much of the confusion in this field results from the lack of universally accepted defining characteristics of the mesenchymal stem cell. A logical proposal for the definition of a marrow mesenchymal stem cell would thus be "a putative marrow cell that cans self-renew and gives rise to a one or more mesenchymal tissues." Murine and human marrow-derived mesenchymal stem cells differentiate into osteoblasts (Ochi et al., 2003), chondrocytes (Imabayashi et al., 2003), skeletal myocytes (Umezawa et al., 1992), adipocytes (Umezawa et al., 1991), and cardiomyocytes (Makino et al., 1999; Takeda et al., 2004) in vitro, and bone marrow-derived mesenchymal cells are a useful cell source for bone regeneration (Ochi et al., 2003) and in vivo cardiovasculogenesis (Gojo et al., 2003). However, marrow derived mesenchymal cells, the population of cells within which the mesenchymal stem cell is thought to exist, can also seemingly differentiate into tissues such as neurons (Kohyama et al., 2001) other than those that originate in the embryonic mesoderm, raising questions about the appropriateness of the term mesenchymal stem cell.

To what extent can the microenvironment, culture conditions, or growth factors dictate the identity of mesenchymal stem cells and their production of different progeny? Serum plays a critical role in the growth of cells in vitro by providing components such as amino acids, lipids, growth factors, vitamins, hormones, and attachment factors, by acting as a pH buffer, and by providing protease inhibitors (Alberts, 2002). Most culture media for mesenchymal cell culture include a poorly defined mixture of macromolecules in the form of fetal calf serum. However, usage of serum for mesenchymal stem cell

culture makes it difficult to know which specific macromolecules a particular type of cell requires to survive and to function normally. This difficulty led to the development of serum-free, chemically defined media. In addition to the usual small molecules, such defined media need to contain growth factors that the mesenchymal stem cells require in culture. The identification of PDGF, EGF, aFGF, LIF, and bFGF as factors essential for the survival, development, and proliferation of mesenchymal stem cells in this study may make it possible to establish minimal conditions under which this cell type behaves in a default state in culture.

Cell growth versus cell life span

We have successfully prolonged the mesenchymal cell life span by introducing the Bmi-1, E6, E7, and TERT genes (Mori et al., 2005; Terai et al., 2005). However, it must be taken into account that even when non-oncogenic genes were introduced for cell-based therapy to increase cell growth and prolong the cell life span. Inhibition of the p16ink4a/Rb pathway is sufficient to prolong the life span of cells in cultures of marrow-derived stroma (Mori et al., 2005). The p16ink4a/Rb pathway is activated in marrow-derived mesenchymal cells in vitro, as in mammary epithelial cells and hepatocytes, but not in foreskin fibroblasts (Kiyono et al., 1998; Simonsen et al., 2002). The development of an appropriate culture system without gene transduction to neutralize the p16ink4a/Rb braking system, that is, stress-free medium for expanding human mesenchymal cells enables us to expand mesenchymal cells almost 100-fold more effectively after 2 weeks of cultivation compared with conventional medium, that is, DMEM supplemented with fetal calf serum.

Growth factor-dependent acceleration of premature senescence or growth arrest is rather unexpected and unfavorable, analogous to pressing down on the gas pedal and the brake pedal simultaneously (Ramirez et al., 2001; Raucci et al., 2004). Up-regulation of cell growth without affecting the cell life span, a key future goal of any cell-based therapy, would thus be an "antinomy" or "trade-off" and put us in a quandary. This can now be achieved by inhibiting the pathway leading to premature senescence without affecting cell proliferation: Signaling from the PDGF receptors by exogenously added PDGF-BB induced p16ink4a protein through p38, and should selectively inhibit the extension of the cell life span without affecting growth factor-dependent cell proliferation through the classical Mek-Erk MAPK pathway (Toyoda et al., 2007). However, this is a challenge to be addressed in the future, probably the not-too-distant future. It is noteworthy again that excessive growth stimulation by growth factors could be one of the cell senescence inducers, like oxidative stress and so-called culture shock (Sherr and DePinho, 2000; Toussaint et al., 2000).

Acknowledgments

We would like to express our sincere thanks to Saito, K., Ishibashi, T., Yamaguchi, T., Terai, M., Sugiki, T., Mori, T., and members of Toyobo for support throughout the work. To view the list of cells used, see http://1985.jukuin.keio.ac.jp/umezawa/cells/name.html.

Literature Cited

Alberts B. 2002. Molecular biology of the cell. New York: Garland Science.
Alcorta DA, Xiong Y, Phelps D, Hannon G, Beach D, Barrett JC. 1996. Involvement of the cyclin-dependent kinase inhibitor p16 (INK4a) in replicative senescence of normal human fibroblasts. Proc Natl Acad Sci USA 93:13742–13747.
Beausejour CM, Krtolica A, Galimi F, Narita M, Lowe SW, Yaswen P, Campisi J. 2003. Reversal of human cellular senescence: Roles of the p53 and p16 pathways. EMBO J 22:4212–4222.
Bébien M, Salinas S, Becamel C, Richard V, Linares L, Hipskind RA. 2003. Immediate-early gene induction by the stresses anisomycin and arsenite in human osteosarcoma cells involves MAPK cascade signaling to Elk-1. CREB and SRF. Oncogene 22:1836–1847.
Campisi J. 2001. From cells to organisms: Can we learn about aging from cells in culture? Exp Gerontol 36:607–618.
Chachques JC, Herreros J, Trainini J, Juffe A, Rendal E, Prosper F, Genovese J. 2004. Autologous human serum for cell culture avoids the implantation of cardioverter-defibrillators in cellular cardiomyoplasty. Int J Cardiol 95:S29–33.
Chen Q, Fischer A, Reagan JD, Yan LJ, Ames BN. 1995. Oxidative DNA damage and senescence of human diploid fibroblast cells. Proc Natl Acad Sci USA 92:4337–4341.
Chen SL, Fang WW, Ye F, Liu YH, Qian J, Shan SJ, Zhang JJ, Chunhua RZ, Liao LM, Lin S, Sun JP. 2004. Effect on left ventricular function of intracoronary transplantation of autologous bone marrow mesenchymal stem cell in patients with acute myocardial infarction. Am J Cardiol 94:92–95.
Gojo S, Gojo N, Takeda Y, Mori T, Abe H, Kyo S, Hata J, Umezawa A. 2003. In vivo cardiovasculogenesis by direct injection of isolated adult mesenchymal stem cells. Exp Cell Res 288:51–59.
Hara E, Smith R, Parry D, Tahara H, Stone S, Peters G. 1996. Regulation of p16CDKN2 expression and its implications for cell immortalization and senescence. Mol Cell Biol 16:859–867.
Hayflick L, Moorhead PS. 1961. The serial cultivation of human diploid cell strains. Exp Cell Res 25:585–621.
Horwitz EM, Prockop DJ, Fitzpatrick LA, Koo WW, Gordon PL, Neel M, Sussman M, Orchard P, Marx JC, Pyeritz RE, Brenner MK. 1999. Transplantability and therapeutic effects of bone marrow-derived mesenchymal cells in children with osteogenesis imperfecta. Nat Med 5:309–313.
Imabayashi H, Mori T, Gojo S, Kiyono T, Sugiyama T, Irie R, Isogai T, Hata J, Toyama Y, Umezawa A. 2003. Redifferentiation of dedifferentiated chondrocytes and chondrogenesis of human bone marrow stromal cells via chondrosphere formation with expression profiling by large-scale cDNA analysis. Exp Cell Res 288:35–50.
Itahana K, Zou Y, Itahana Y, Martinez JL, Beausejour C, Jacobs JJ, Van Lohuizen M, Band V, Campisi J, Dimri GP. 2003. Control of the replicative life span of human fibroblasts by p16 and the polycomb protein Bmi-1. Mol Cell Biol 23:389–401.
Iwasa H, Han J, Ishikawa F. 2003. Mitogen-activated protein kinase p38 defines the common senescence-signalling pathway. Genes Cells 8:131–144.
Jaquet K, Krause KT, Denschel J, Faessler P, Nauerz M, Geidel S, Boczor S, Lange C, Stute N, Zander A, Kuck KH. 2005. Reduction of myocardial scar size after implantation of mesenchymal stem cells in rats: What is the mechanism? Stem Cells Dev 14:299–399.
Kiyono T, Foster SA, Koop JI, McDougall JK, Galloway DA, Klingelhutz AJ. 1998. Both Rb/p16INK4a inactivation and telomerase activity are required to immortalize human epithelial cells. Nature 396:84–88.
Koç ON, Gerson SL, Cooper BW, Dyhouse SM, Haynesworth SE, Caplan AI, Lazarus HM. 2000. Rapid hematopoietic recovery after coinfusion of autologous-blood stem cells and culture-expanded marrow mesenchymal stem cells in advanced breast cancer patients receiving high-dose chemotherapy. J Clin Oncol 18:307–316.
Koç ON, Day J, Nieder M, Gerson SL, Lazarus HM, Krivit W. 2002. Allogeneic mesenchymal stem cell infusion for treatment of metachromatic leukodystrophy (MLD) and Hurler syndrome (MPS-IH). Bone Marrow Transplant 30:215–222.
Kohyama J, Abe H, Shimazaki T, Koizumi A, Nakashima K, Gojo S, Taga T, Okano H, Hata J, Umezawa A. 2001. Brain from bone: Efficient "meta-differentiation" of marrow stroma-derived mature osteoblasts to neurons with Noggin or a demethylating agent. Differentiation 68:235–244.
Kopen GCPD, Phinney DG. 1999. Marrow stromal cells migrate throughout forebrain and cerebellum, and they differentiate into astrocytes after injection into neonatal mouse brains. Proc Natl Acad Sci USA 96:10711–10716.
Lange C, Tögel F, Ittrich H, Clayton F, Nolte-Ernsting C, Zander AR, Westenfelder C. 2005. Administered mesenchymal stem cells enhance recovery from ischemia/reperfusion-induced acute renal failure in rats. Kidney Int 68.
Lange C, Cakiroglu F, Spiess AN, Cappallo-Obermann H, Dierlamm J, Zander AR. 2007. Accelerated and safe expansion of human mesenchymal stromal cells in animal serum-free medium for transplantation and regenerative medicine. J Cell Physiol 213:18–26.
Le Blanc K, Rasmusson I, Sundberg B, Götherström C, Hassan M, Uzunel M, Ringdén O. 2004. Treatment of severe acute graft-versus-host disease with third party haploidentical mesenchymal stem cells. Lancet 363:1439–1441.
Lennon DP, Haynesworth SE, Young RG, Dennis JE, Caplan AI. 1995. A chemically defined medium supports in vitro proliferation and maintains the osteochondral potential of rat marrow-derived mesenchymal stem cells. Exp Cell Res 219:211–222.
Lin AW, Barradas M, Stone JC, van Aelst L, Serrano M, Lowe SW. 1998. Premature senescence involving p53 and p16 is activated in response to constitutive MEK/MAPK mitogenic signaling. Genes Dev 12:3008–3019.
Mahmood A, Lu D, Chopp M. 2004. Marrow stromal cell transplantation after traumatic brain injury promotes cellular proliferation within the brain. Neurosurgery 55:1185–1193.
Makino S, Fukuda K, Miyoshi S, Konishi F, Kodama H, Pan J, Sano M, Takahashi T, Hori S, Abe H, Hata J, Umezawa A, Ogawa S. 1999. Cardiomyocytes can be generated from marrow stromal cells in vitro. J Clin Invest 103:697–705.
Martin MJ, Muotri A, Gage F, Varki A. 2005. Human embryonic stem cells express an immunogenic nonhuman sialic acid. Nat Med 11:228–232.
Mori T, Kiyono T, Imabayashi H, Takeda Y, Tsuchiya K, Miyoshi S, Makino H, Matsumoto K, Saito H, Ogawa S, Sakamoto M, Hata J, Umezawa A. 2005. Combination of hTERT and bmi-1, E6, or E7 induces prolongation of the life span of bone marrow stromal cells from an elderly donor without affecting their neurogenic potential. Mol Cell Biol 25:5183–5195.
Ng F, Boucher S, Koh S, Sastry KS, Chase L, Lakshmipathy U, Choong C, Yang Z, Vemuri MC, Rao MS, Tanavde V. 2008. PDGF, TGF-beta, and FGF signaling is important for differentiation and growth of mesenchymal stem cells (MSCs): Transcriptional profiling can identify markers and signaling pathways important in differentiation of MSCs into adipogenic, chondrogenic, and osteogenic lineages. Blood 112:295–307.
Ochi K, Chen G, Ushida T, Gojo S, Segawa K, Tai H, Ueno K, Ohkawa H, Mori T, Yamaguchi A, Toyama Y, Hata J, Umezawa A. 2003. Use of isolated mature osteoblasts in abundance acts as desired-shaped bone regeneration in combination with a modified poly-DL-lactic-co-glycolic acid (PLGA)-collagen sponge. J Cell Physiol 194:45–53.
Parrinello S, Samper E, Krtolica A, Goldstein J, Melov S, Campisi J. 2003. Oxygen sensitivity severely limits the replicative lifespan of murine fibroblasts. Nat Cell Biol 5:741–747.
Petite H, Viateau V, Bensaïd W, Meunier A, de Pollak C, Bourguignon M, Oudina K, Sedel L, Guillemin G. 2000. Tissue-engineered bone regeneration. Nat Biotechnol 18:959–963.
Pittenger MF, Mackay AM, Beck SC, Jaiswal RK, Douglas R, Mosca JD, Moorman MA, Simonetti DW, Craig S, Marshak DR. 1999. Multilineage potential of adult human mesenchymal stem cells. Science 284:143–147.
Ramirez RD, Morales CP, Herbert BS, Rohde JM, Passons C, Shay JW, Wright WE. 2001. Putative telomere-independent mechanisms of replicative aging reflect inadequate growth conditions. Genes Dev 15:398–403.

Raucci A, Laplantine E, Mansukhani A, Basilico C. 2004. Activation of the ERK1/2 and p38 mitogen-activated protein kinase pathways mediates fibroblast growth factor-induced growth arrest of chondrocytes. J Biol Chem 279:1747–1756.

Rheinwald JG, Hahn WC, Ramsey MR, Wu JY, Guo Z, Tsao H, De Luca M, Catricala C, O'Toole KM. 2002. A two-stage, p16(INK4A)- and p53-dependent keratinocyte senescence mechanism that limits replicative potential independent of telomere status. Mol Cell Biol 22:5157–5172.

Sano M, Umezawa A, Abe H, Akatsuka A, Nonaka S, Shimizu H, Fukuma M, Hata J. 2001. EAT/mcl-1 expression in the human embryonal carcinoma cells undergoing differentiation or apoptosis. Exp Cell Res 266:114–125.

Schichor C, Birnbaum T, Etminan N, Schnell O, Grau S, Miebach S, Aboody K, Padovan C, Straube A, Tonn JC, Goldbrunner R. 2006. Vascular endothelial growth factor A contributes to glioma-induced migration of human marrow stromal cells (hMSC). Exp Neurol 199:301–310.

Seifert RA, van Koppen A, Bowen-Pope DF. 1993. PDGF-AB requires PDGF receptor alpha-subunits for high-affinity, but not for low-affinity, binding and signal transduction. J Biol Chem 268:4473–4480.

Selvaggi TA, Walker RE, Fleisher TA. 1997. Development of antibodies to fetal calf serum with arthus-like reactions in human immunodeficiency virus-infected patients given syngeneic lymphocyte infusions. Blood 89:776–779.

Serrano M. 1997. The tumor suppressor protein p16INK4a. Exp Cell Res 237:7–13.

Sherr CJ, DePinho RA. 2000. Cellular senescence: Mitotic clock or culture shock? Cell 102:407–410.

Shimo T, Matsumura S, Ibaragi S, Isowa S, Kishimoto K, Mese H, Nishiyama A, Sasaki A. 2007. Specific inhibitor of MEK-mediated cross-talk between ERK and p38 MAPK during differentiation of human osteosarcoma cells. J Cell Commun Signal 1:103–111.

Simonsen JL, Rosada C, Serakinci N, Justesen J, Stenderup K, Rattan SI, Jensen TG, Kassem M. 2002. Telomerase expression extends the proliferative life-span and maintains the osteogenic potential of human bone marrow stromal cells. Nat Biotechnol 20:592–596.

Takeda Y, Mori T, Imabayashi H, Kiyono T, Gojo S, Miyoshi S, Hida N, Ita M, Segawa K, Ogawa S, Sakamoto M, Nakamura S, Umezawa A. 2004. Can the life span of human marrow stromal cells be prolonged by bmi-1, E6, E7, and/or telomerase without affecting cardiomyogenic differentiation? J Gene Med 6:833–845.

Tamama K, Fan VH, Griffith LG, Blair HC, Wells A. 2006. Epidermal growth factor as a candidate for ex vivo expansion of bone marrow-derived mesenchymal stem cells. Stem Cells (Dayton, Ohio) 24:686–695.

Terai M, Uyama T, Sugiki T, Li XK, Umezawa A, Kiyono T. 2005. Immortalization of human fetal cells: The life span of umbilical cord blood-derived cells can be prolonged without manipulating p16INK4a/RB braking pathway. Mol Biol Cell 16:1491–1499.

Tögel F, Hu Z, Weiss K, Isaac J, Lange C, Westenfelder C. 2005. Administered mesenchymal stem cells enhance recovery from ischemia/reperfusion-induced acute renal failure in rats. Am J Physiol Renal Physiol 289:F31–F42.

Toussaint O, Medrano EE, von Zglinicki T. 2000. Cellular and molecular mechanisms of stress-induced premature senescence (SIPS) of human diploid fibroblasts and melanocytes. Exp Gerontol 35:927–945.

Toyoda M, Takahashi H, Umezawa A. 2007. Ways for a mesenchymal stem cell to live on its own: Maintaining an undifferentiated state ex vivo. Int J Hematol 86:1–4.

Tropepe V, Hitoshi S, Sirard C, Mak TW, Rossant J, van der Kooy D. 2001. Direct neural fate specification from embryonic stem cells: A primitive mammalian neural stem cell stage acquired through a default mechanism. Neuron 30:65–78.

Umezawa A, Tachibana K, Harigaya K, Kusakari S, Kato S, Watanabe Y, Takano T. 1991. Colony-stimulating factor 1 expression is down-regulated during the adipocyte differentiation of H-1/A marrow stromal cells and induced by cachectin/tumor necrosis factor. Mol Cell Biol 11:920–927.

Umezawa A, Maruyama T, Segawa K, Shadduck RK, Waheed A, Hata J. 1992. Multipotent marrow stromal cell line is able to induce hematopoiesis in vivo. J Cell Physiol 151:197–205.

Wang W, Chen JX, Liao R, Deng Q, Zhou JJ, Huang S, Sun P. 2002. Sequential activation of the MEK-extracellular signal-regulated kinase and MKK3/6-p38 mitogen-activated protein kinase pathways mediates oncogenic ras-induced premature senescence. Mol Cell Biol 22:3389–3403.

Wei W, Sedivy JM. 1999. Differentiation between senescence (M1) and crisis (M2) in human fibroblast cultures. Exp Cell Res 253:519–522.

Wiles MV, Johansson BM. 1999. Embryonic stem cell development in a chemically defined medium. Exp Cell Res 247:241–248.

Williamson AJ, Dibling BC, Boyne JR, Selby P, Burchill SA. 2004. Basic fibroblast growth factor-induced cell death is effected through sustained activation of p38MAPK and up-regulation of the death receptor p75NTR. J Biol Chem 279:47912–47928.

Yao CL, Chu IM, Hsieh TB, Hwang SM. 2004. A systematic strategy to optimize ex vivo expansion medium for human hematopoietic stem cells derived from umbilical cord blood mononuclear cells. Exp Hematol 32:720–727.

EXPERIMENTAL CELL RESEARCH 315 (2009) 2727-2740

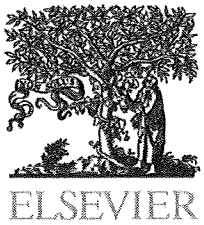

101種類のヒトiPS作製(図5)を発表した論文

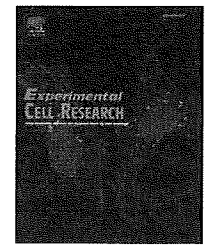

Research Article

Mesenchymal to embryonic incomplete transition of human cells by chimeric OCT4/3 (POU5F1) with physiological co-activator EWS

Hatsune Makino[a], *Masashi Toyoda*[a], *Kenji Matsumoto*[b], *Hirohisa Saito*[b], *Koichiro Nishino*[a], *Yoshihiro Fukawatase*[a], *Masakazu Machida*[a], *Hidenori Akutsu*[a], *Taro Uyama*[a], *Yoshitaka Miyagawa*[c], *Hajime Okita*[c], *Nobutaka Kiyokawa*[c], *Takashi Fujino*[d,f], *Yuichi Ishikawa*[e], *Takuro Nakamura*[d], *Akihiro Umezawa*[a,*]

[a] *Department of Reproductive Biology, National Institute for Child Health and Development, Tokyo, 157-8535, Japan*
[b] *Department of Allergy and Immunology, National Institute for Child Health and Development, Tokyo, 157-8535, Japan*
[c] *Department of Developmental Biology and Pathology, National Institute for Child Health and Development, Tokyo, 157-8535, Japan*
[d] *Department of Carcinogenesis, The Cancer Institute, Japanese Foundation for Cancer Research, Tokyo, 140-8455, Japan*
[e] *Department of Pathology, The Cancer Institute, Japanese Foundation for Cancer Research, Tokyo, 140-8455, Japan*
[f] *Department of Pathology, Faculty of Medicine, Kyorin University, Tokyo, 181-8611, Japan*

ARTICLE INFORMATION

Article Chronology:
Received 7 November 2008
Revised version received 15 June 2009
Accepted 16 June 2009
Available online 24 June 2009

Keywords:
Dedifferentiation
Mesoderm
Embryonic carcinoma
iPS cell
OCT4/3
Stem cell

ABSTRACT

POU5F1 (more commonly known as OCT4/3) is one of the stem cell markers, and affects direction of differentiation in embryonic stem cells. To investigate whether cells of mesenchymal origin acquire embryonic phenotypes, we generated human cells of mesodermal origin with overexpression of the chimeric *OCT4/3* gene with physiological co-activator EWS (product of the *EWSR1* gene), which is driven by the potent *EWS* promoter by translocation. The cells expressed embryonic stem cell genes such as *NANOG*, lost mesenchymal phenotypes, and exhibited embryonal stem cell-like alveolar structures when implanted into the subcutaneous tissue of immunodeficient mice. Hierarchical analysis by microchip analysis and cell surface analysis revealed that the cells are subcategorized into the group of human embryonic stem cells and embryonal carcinoma cells. These results imply that cells of mesenchymal origin can be traced back to cells of embryonic phenotype by the *OCT4/3* gene in collaboration with the potent cis-regulatory element and the fused co-activator. The cells generated in this study with overexpression of chimeric OCT4/3 provide us with insight into cell plasticity involving OCT4/3 that is essential for embryonic cell maintenance, and the complexity required for changing cellular identity.

Introduction

Somatic stem cells have been shown to have a more flexible potential, but the conversion of mesenchymal cells to embryonic stem (ES) cells has still been a challenge and requires gene transduction [1–4]. This phenotypic conversion requires the molecular reprogramming of mesenchyme. Mesenchymal stem cells or mesenchymal progenitors have been isolated from adult bone marrow [5], adipose tissue [6], dermis [7], endometrium [8], menstrual blood [8], cord blood [9,10], and other connective tissues [11]. These cells are

* *Corresponding author.* Fax: +81 3 5494 7048.
E-mail address: umezawa@1985.jukuin.keio.ac.jp (A. Umezawa).

0014-4827/$ – see front matter © 2009 Elsevier Inc. All rights reserved.
doi:10.1016/j.yexcr.2009.06.016

capable of differentiating into osteoblasts [12], chondrocytes [13], skeletal myocytes, adipocytes, cardiomyocytes [14,15], and neural cells [16]. However, most of the differentiation capability is limited to cells of mesodermal origin. This is in contrast to ES cells derived from the inner cell mass of the blastocyst that differentiate into cells of three germ cell layers. ES cells are pluripotent and immortal, and, therefore, ES cells provide an unlimited number of specialized cells.

Embryonic and adult fibroblasts have been induced to become pluripotent stem cells (iPS cells) or ES-like cells by defined factors including POU5F1 (also known as OCT4/3) [1–3]. OCT4/3 protein, a member of the POU family of transcription factors, is related to the pluripotent capacity of ES cells, and is thus a distinctive marker to identify primordial germ and embryonic stem cells [17–21]. OCT4/3 is down-regulated during oogenesis and spermatogenesis [22]. Furthermore, knocking out the *OCT4/3* gene in mice causes early lethality because of lack of inner cell mass formation [23], and OCT4/3 is critical for self-renewal of ES cells [24]. During human development, expression of OCT4/3 is found at least until the blastocyst stage [25] in which it is involved in gene expression regulation. OCT4/3 functions as a master switch in differentiation by regulating cells that have, or can develop, pluripotent potential by activating transcription via octamer motifs [26].

The EWS gene was originally identified at the chromosomal translocation, and fused with the ets transcription factors in Ewing sarcoma, as is the case of other sarcomas [27–30].

We report here the generation of human cells that overexpress the *OCT4/3* gene with physiological co-activator EWS (translation product of the *EWS* gene). In this study we show that the cells of mesenchymal origin overexpressing OCT4/3 can be traced back to cells with an embryonic phenotype.

Materials and methods

Cell culture

GBS6 cells were generated from primary or first passage cells of a pelvic tumor [31], and cultured in tissue culture dishes (100 mm, Becton Dickinson) in the G031101 medium (Med Shirotori, Tokyo). All cultures were maintained at 37 °C in a humidified atmosphere containing 95% air and 5% CO_2. When the cultures reached subconfluence, the cells were harvested with Trypsin–EDTA Solution (cat# 23315, IBL) at 0.06% trypsin, and replated at a density of 5×10^5 in a 100 mm dish. Medium changes were carried out twice weekly thereafter. Both H4-1 and Yub10F were human bone marrow cells. The 3F0664 were human bone marrow-derived mesenchymal cells and were purchased from Lonza (PT-2501, Basel, Switzerland). The H4-1, Yub10F and 3F0664 cells were cultured in the mesenchymal-stem-cell-growth (MSCG)-Medium-BulletKit (PT-3001, Lonza). The NCR-G1 (a human yolk sac tumor line), NCR-G2 (a human embryonal carcinoma cell line from a testicular tumor), NCR-G3 (a human embryonal carcinoma cell line from a testicular tumor) and NCR-G4 (a human embryonal carcinoma cell line) were cultured in the G031101 medium as previously described [32]. In an experiment to inhibit cell adhesion, GBS6 and NCR-G3 cells were treated with anti-human E-cadherin, monoclonal (Clone HECD-1) (M106, TAKARA BIO INC.) at 100 μg/mL. Treatment with the demethylating agent, 5′-aza-2′-deoxycytidine (5azaC; A2385, SIGMA), was performed on GBS6 cells. GBS6 cells were treated with 3 μM of 5azaC for 24 h, and then cultured without treatment for 24 h. The 5azaC-traeated GBS6 cells were described as "GBS6-5azaC". MRC-5 human fetal lung fibroblasts were maintained in POWEREDBY10 medium (MED SHIROTORI CO., Ltd, Tokyo, Japan). We used these cells at between 17 and 25 PDs for the infection of the retroviral vectors. 293FT cells were maintained in DMEM containing 10% FBS, 1% penicillin and streptomycin. iPS cells were maintained in iPSellon medium (007001, Cardio) supplemented with 10 ng/mL recombinant human basic fibroblast growth factor (bFGF, WAKO, Japan). For passaging, iPS cells were washed once with PBS and then incubated with Dulbecco's Phosphate-Buffered Saline (14190-144, Invitrogen) containing 1 mg/mL Collagenase IV (17104-019, Invitrogen), 1 mM $CaCl_2$, 20% Knockout Serum Replacement (KSR) (10828-028, Invitrogen), and 0.05% Trypsin–EDTA Solution (23315, IBL) at 37 °C. When colonies at the edge of the dish started dissociating from the bottom, DMEM/F12/collangenase was removed. Cells were scraped and collected into 15 mL conical tubes. An appropriate volume of the medium was added, and the contents were transferred to a new dish on irradiated MEF feeder cells. The split ratio was routinely 1:3.

G-banding karyotypic analysis and spectral karyotyping (SKY) analysis

Metaphase spreads were prepared from cells treated with Colcemid (Karyo Max, Gibco Co. BRL, 100 ng/mL for 6 h). We performed a standard G-banding karyotypic analysis on at least 50 metaphase spreads for each population. SKY analysis was performed on metaphase-transduced cells according to the kit manufacturer's instruction (ASI, Carlsbad, CA) and a previously published method [33].

RT-PCR

The cDNAs were synthesized with an aliquot (5 μg) of each total RNA using Oligo-(dT)20 primer (18418-020, Invitrogen) and SuperScript III Reverse Transcriptase (18080-044, Invitrogen). Both the RNA strand of an RNA–DNA hybrid and single-stranded DNA were degraded by RNaseH (18021-071, Invitrogen). For the thermal cycle reactions, cDNA was amplified by T3 Thermocycler (Biometra, Goettingen, Germany) under the following reaction conditions: 30 cycles of a PCR (94 °C for 30 s, 55 °C for 30 s and 72 °C for 30 s) after an initial denaturation (94 °C for 1 min). Primer sets used for PCR reactions are described in Tables 1 and 2. As the same amount of cDNA template was used in all reactions, in comparison to the glyceraldehyde-3-phosphate dehydrogenase (GAPDH) standard, the expression levels were evaluated. The controls consisted of reactions without reverse transcriptase in the process of cDNA synthesis.

Table 1 – PCR primers to detect the chimeric *EWS-OCT4/3* gene and untranslocated *OCT4/3* gene.

Symbol	Name	Sequence
A	EWS exon6-F	5′ TTA GAC CGC AGG ATG GAA AC 3′
B	EWS ex6 intron-F	5′ GTG GGG TTC ACT AT 3′
C	POU5F1-1a-F	5′ GAT CCT CGG ACC TGG CTA AG 3′
D	POU5F1-2-F	5′ CTT GCT GCA GAA GTG GGT GGA GGA A 3′
E	POU5F1-1a-R	5′ TCA GGC TGA GAG GTC TCC AA 3′
F	POU5F1-3-R	5′ CTG CAG TGT GGG TTT CGG GCA 3′

Table 2 – PCR primers for detection of gene transcripts.

Name	Sequence	Size (bp)
Nanog	Forward: 5′ AGT CCC AAA GGC AAA CAA CCC ACT TC 3′ Reverse: 5′ ATC TGC TGG AGG CTG AGG TAT TTC TGT CTC 3′	164
Sox2	Forward: 5′ ACC GGC GGC AAC CAG AAG AAC AG 3′ Reverse: 5′ GCG CCG CGG CCG GTA TTT AT 3′	253
UTF1	Forward: 5′ ACC AGC TGC TGA CCT TGA AC 3′ Reverse: 5′ TTG AAC GTA CCC AAG AAC GA 3′	230
GAPDH	Forward: 5′ GCT CAG ACA CCA TGG GGA AGG T 3′ Reverse: 5′ GTG GTG CAG GAG GCA TTG CTG A 3′	474

Immunoblot analysis

Whole lysates of GBS6 or NCR-G3 cells were loaded on 10% SDS/PAGE (40 μg total protein/lane) and transferred to a nitrocellulose membrane. The blots were probed with antibodies against anti-Oct3/4 (C-20 for the C-terminus of OCT4/3 of human origin; sc-8629, Santa Cruz), developed with polyclonal rabbit anti-goat Immunoglobulins/HRP antibody (P0160; Dako), and detected by chemiluminescence following the manufacturer's protocol (ECL Western Blotting Analysis System, Amersham).

Flow cytometric analysis

Cells were stained for 30 min at 4 °C with primary antibodies and immunofluorescent secondary antibodies. The cells were then analyzed on a Cytomics FC 500 (Beckman Coulter, Inc., Fullerton, CA, USA) and the data were analyzed with the FC500 CXP Software ver.2.0 (Beckman Coulter, Inc., Fullerton, CA, USA). Antibodies against human CD9 (555372, PharMingen), CD13 (IM0778, Beckman), CD14 (6603511, Beckman), CD24 (555426, PharMingen), CD29 (6604105, PharMingen), CD31 (IM1431, Beckman), CD34 (IM1250, Beckman), CD44 (IM1219, Beckman), CD45 (556828, PharMingen), CD50 (IM1601, Beckman), CD55 (IM2725, Beckman), CD59 (IMK3457, Beckman), CD73 (550257, PharMingen), CD81 (555676, PharMingen), CD90 (IM1839, Beckman), CD105 (A07414, Beckman), CD106 (IM1244, Beckman), CD117 (IM1360, Beckman), CD130 (555756, PharMingen), CD133 (130-080-801, Miltenyi Biotec), CD135 (IM2234, Beckman), CD140a (556002, PharMingen), CD140b (558821, PharMingen), CD157 (D036-3, IBL), CD166 (559263, PharMingen), CD243 (IM2370, Beckman), ABCG2 (K0027-3, IBL),

Table 3 – Expression of human ES cell-associated genes.

A

Cell		OCT4/3	SOX2	NANOG	UTF1	TDGF1	ZIC3	DPPA4	MYC	KLF4
GBS6	Flags	P	A	A	A	A	A	A	P	A
	Raw	2493	56	9	15	23	19	9	3261	171
GBS6-5azaC	Flags	P	A	A	A	A	A	A	P	A
	Raw	6620	146	19	28	20	15	11	1359	102
NCR-G1	Flags	A	A	A	A	P	P	A	A	A
	Raw	46	67	11	19	5180	2349	97	157	91
NCR-G2	Flags	P	A	P	A	P	P	P	A	A
	Raw	2093	120	3972	166	2154	389	873	160	84
NCR-G3	Flags	P	P	P	P	P	P	P	P	P
	Raw	14338	1239	14925	9208	11207	5294	4036	1086	1151
NCR-G4	Flags	P	P	P	P	P	P	P	P	A
	Raw	10602	352	9469	1684	9830	2741	2138	746	151
H4-1	Flags	A	A	A	A	A	A	A	P	P
	Raw	83	13	11	17	40	7	2	1635	489
3F0664	Flags	A	A	A	A	A	A	A	P	P
	Raw	56	63	14	34	21	21	22	735	832
Yub10F	Flags	A	A	A	A	A	A	A	P	A
	Raw	19	49	9	63	12	12	4	680	9

B

Gene symbol	Probe set ID	Gene name
POU5F1	208286_x_at	Oct4/3
SOX2	213721_at	Sox2
NANOG	220184_at	Nanog; Nanog homeobox
UTF1	208275_x_at	Utf1; undifferentiated embryonic cell transcription factor 1
TDGF1	206286_s_at	Tdgf1; teratocarcinoma-derived growth factor 1
ZIC3	207197_at	Zic3; odd-paired homolog
DPPA4	219651_at	Dppa4; developmental pluripotency associated 4
MYC	202431_s_at	c-myc
KLF4	220266_s_at	Klf4; Kruppel-like factor 4

A. Gene expression was examined with the Human Genome U133A Probe array (Affymetrix). Raw data values (*Raw*) for each gene expression are shown. *Flags*: Gene expression was judged to be "*P* (present)" or "*A* (absent)" in each cell by the GeneChip Analysis Suite 5.0 computer program. GBS6-5azaC: GBS6 cells were exposed to 3 μM 5′-aza-2′-deoxycytidine for 24 h, and then cultured without any treatment for 24 h.
B. Gene names for each symbol.

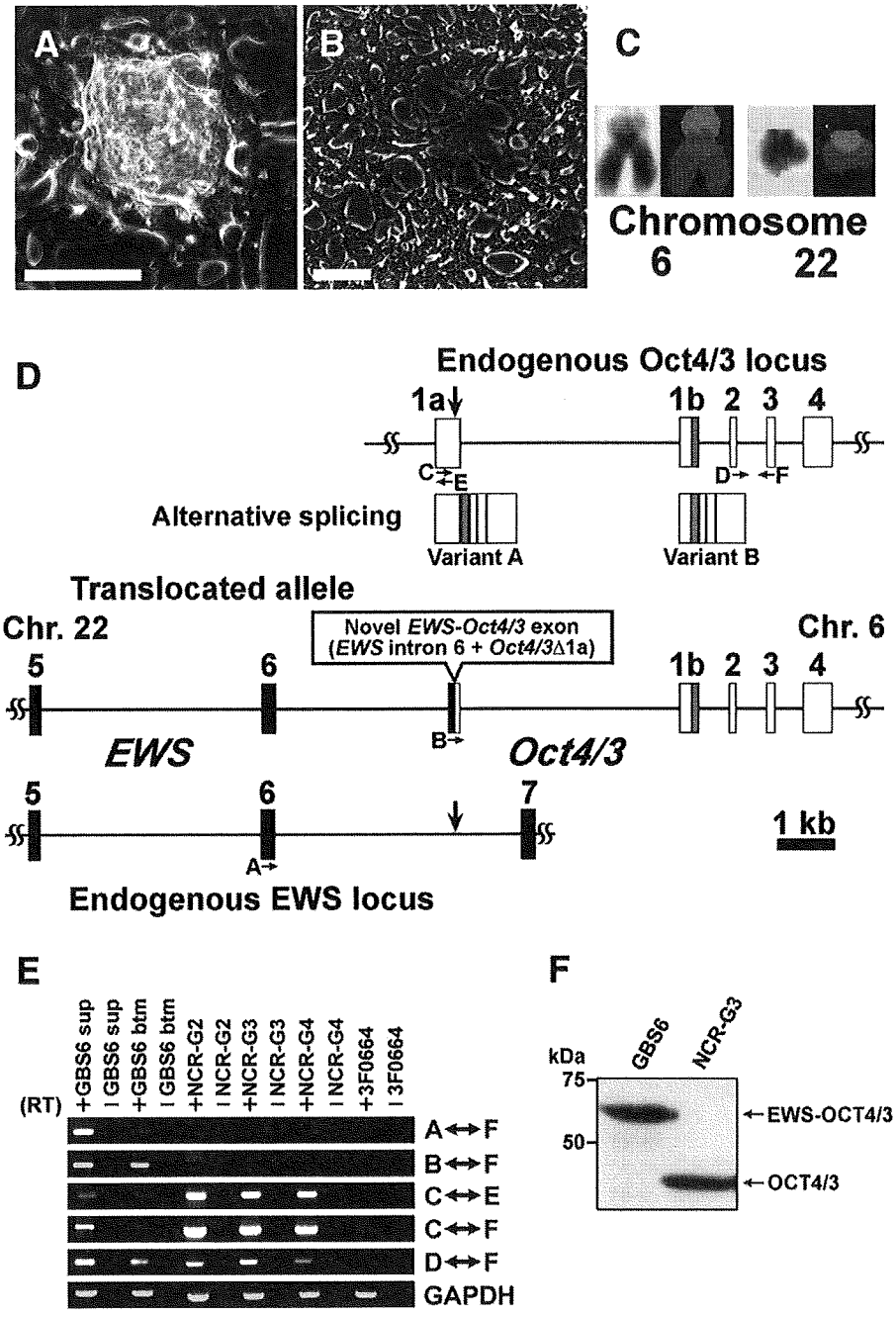

Fig. 1 – Phase contrast micrograph of GBS6 cells, and expression of the translocated *POU5F1/OCT4/3* gene. A cell line termed "GBS6" was generated from primary or first passage cells of a pelvic tumor [31]. (A) GBS6 cell aggregate (GBS6 sup). Scale bar: 100 μm. (B) GBS6 adherent cells (GBS6 btm). Scale bar: 100 μm. (C) G-banding karyotypic analysis and Spectral karyotyping (SKY) analysis of the translocated chromosomes. (D) Schematic representation of the *EWS-OCT4/3* structure in the t(6;22) tumor. *EWS* exons are represented by black boxes and *OCT4/3* exons by open boxes. The *OCT4/3*-1b exon is composed of an open and gray box. The novel *EWS-OCT4/3* chimeric exon is created by the fusion between *EWS* intron 6 and part of the exon of *OCT4/3* (Δ1a). The vertical arrows indicate each breakpoint on either chromosome 22 (*EWS*) or chromosome 6 (*OCT4/3*). The horizontal arrows indicate the position and direction of primers for PCR (Table 1). (E) RT-PCR analysis of the translocated *OCT4/3* gene and the untranslocated *OCT4/3* gene in GBS6 cell, NCR-G2, NCR-G3, NCR-G4, and 3F0664 cells. NCR-G2, NCR-G3, and NCR-G4 cells are embryonal carcinoma cells, and 3F0664 cells are mesenchymal cells. (F) Western blot analysis of EWS-OCT4/3 in GBS6 cells. Western blot analysis was performed using anti-Oct4/3 antibody. EWS-OCT4/3 chimeric protein (~58 kDa) was detected in GBS6 cells. The positions of prestained molecular markers (BIO-RAD) are indicated to the left (kDa).

HLA-ABC (IM1838, Beckman), HLA-DR, DP, DQ (6604366, Beckman), SSEA-1 (MAB4301, Chemicon), SSEA-3 (MAB4303, Chemicon), SSEA-4 (MAB4304, Chemicon), STRO-1 (MAB1038, R and D Systems), TRA-1-60 (MAB4360, Chemicon), and TRA-1-81 (MAB4381, Chemicon) were adopted as primary antibodies. PE-conjugated anti-mouse Ig antibody (550589, Pharmingen), PE-conjugated anti-mouse IgM antibody (555584, Pharmingen) and PE-conjugated anti-rat Ig antibody (550767, Pharmingen) were used as secondary antibodies. X-Mean, the sum of the intensity divided by total cell number, was automatically calculated, and it was adopted for the evaluation of this experiment.

Implantation of cells into mice

GBS6 cells ($>1\times10^7$) were subcutaneously inoculated into an immunodeficient, NOD/Shi-*scid*, IL-2Rγ^{null} mouse (NOG mouse) (CREA, Tokyo, Japan). Subcutaneous specimens were resected at 2 weeks after implantation. The operation protocols were accepted by the Laboratory Animal Care and the Use Committee of the National Research Institute for Child and Health Development, Tokyo (approval number: 2003-002 and 2005-003).

Immunohistochemistry analysis

Immunohistochemical analysis was performed as previously described [34–36] with antibodies to MIC2 (clone# 12E7, cat# M3601, DAKO, Carpinteria, CA, USA), vimentin (clone# V9, cat# M0725, DAKO, Carpinteria, CA, USA), neurofilament protein 70 kDa (NF-L, clone# 2F11, cat# M0762, DAKO, Carpinteria, CA, USA), desmin (clone# D9, cat# 010031, Bio-Science Products AG, Emmenbruecke, Switzerland), smooth muscle actin (clone# 1A4, cat# M0851, DAKO, Carpinteria, CA, USA), and OCT4/3 (clone# C-10, cat# sc-5279, Santa Cruz Biotechnology, Inc., CA, USA) in PBS containing 1% bovine serum albumin. As a methodological control, the primary antibody was omitted. Immunohistochemical analysis of iPS cells was performed according to the manufacturer's protocol [SCR002,

A

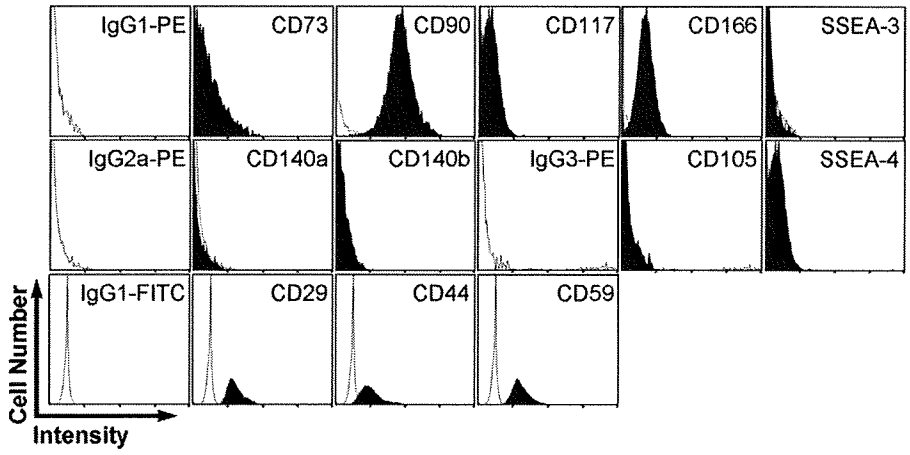

B

Negative (y≦0.1)			Low (0.1<y<1)	Positive (1<y)
CD13	CD106	ABCG2	CD73	CD9
CD14	CD117	HLA-DR,DQ,DP	CD166	CD29
CD24	CD130	SSEA-1		CD44
CD31	CD133	SSEA-3		CD59
CD34	CD135	SSEA-4		CD81
CD45	CD140a	Stro-1		CD90
CD50	CD140b	TRA-1-60		HLA-A,B,C
CD55	CD157	TRA-1-81		
CD105	CD243			

Fig. 2 – Cell surface marker analysis of GBS6 cells. (A) Flow cytometric analysis of cell surface markers in GBS6 cells. The results of CD73, CD90, CD117, CD166 and SSEA-3 were compared with the result of their isotype control, PE-conjugated IgG1. The results of CD140a and CD140b were compared with the result of PE-conjugated IgG2a. The results of CD105 and SSEA-4 were compared with the result of PE-conjugated IgG3. The results of CD29, CD44 and CD59 were compared with the result of FITC-conjugated IgG1. *X*-axis and *Y*-axis indicate the intensity and the cell number, respectively. (B) Summary of cell surface markers. "*y*" is "X-means" subtracted by 'a value of isotype control'; "$y<0.1$", "$0.1<y<1$", and "$1<y$" were determined "negative", "low" and "positive", respectively.

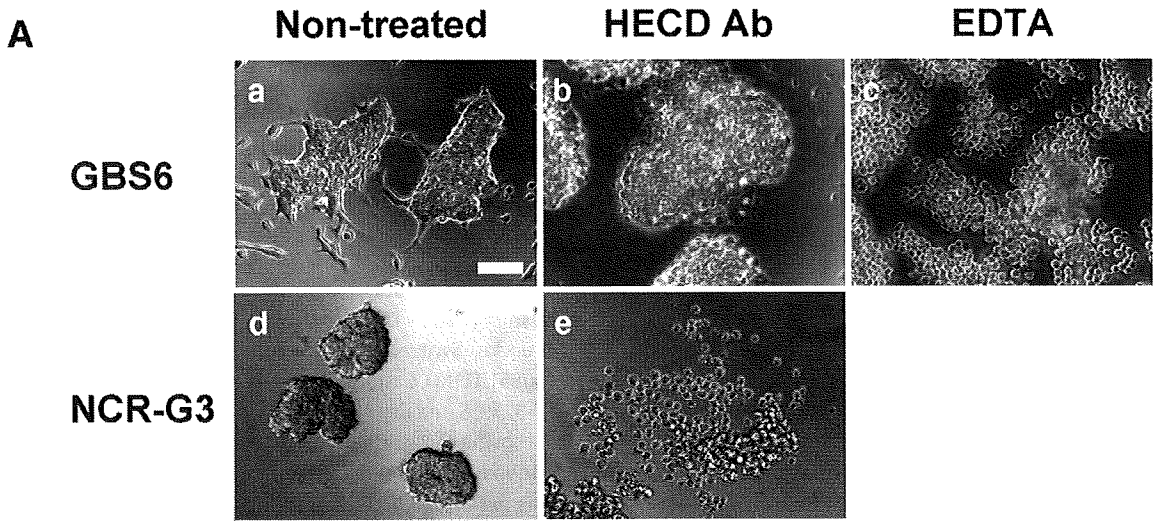
A
Non-treated
HECD Ab
EDTA
GBS6
NCR-G3
a
b
c
d
e

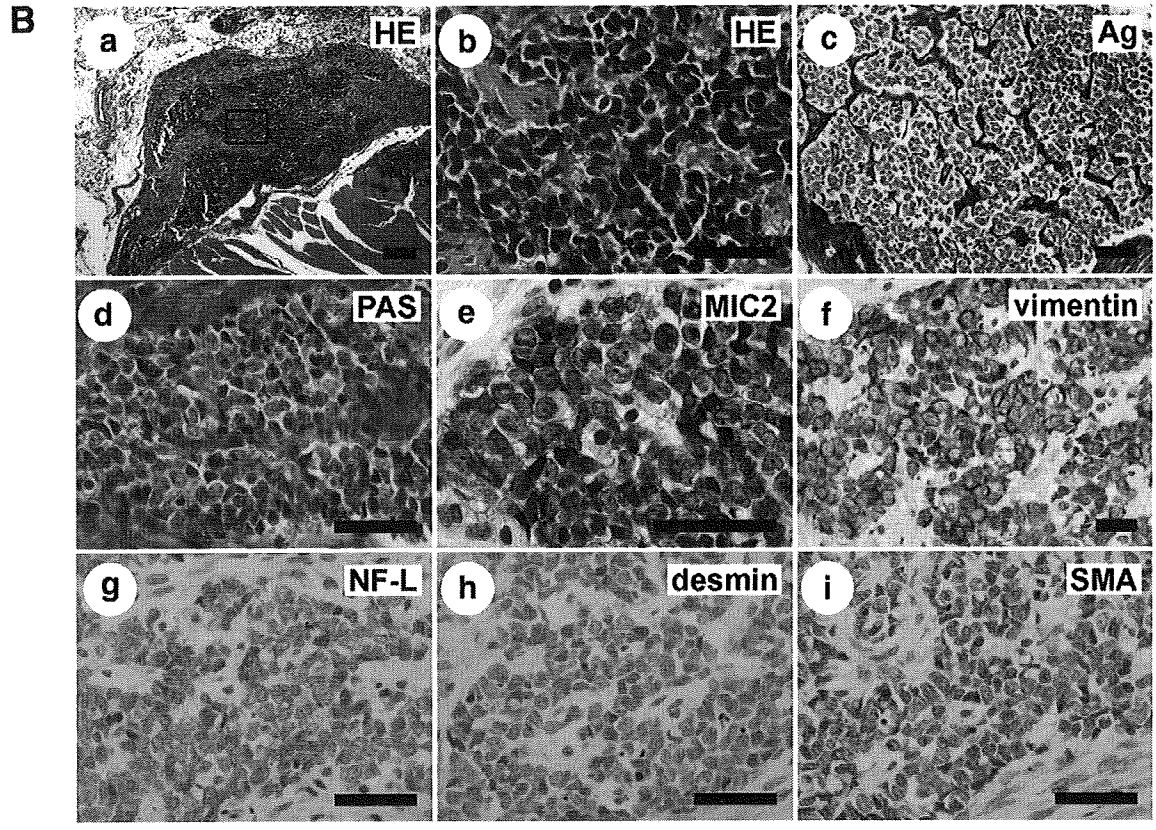
B
a HE
b HE
c Ag
d PAS
e MIC2
f vimentin
g NF-L
h desmin
i SMA

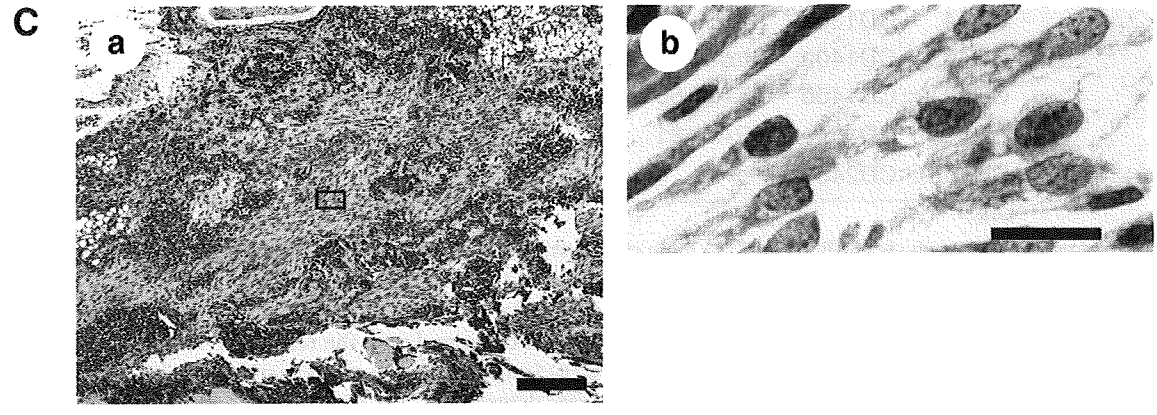
C
a
b

Chemicon (Millipore)]. Primary antibodies included Oct-3/4 (C-10) (diluted at 1:300, sc-5279, Santa Cruz), NANOG (diluted at 1:300, RCAB0003P, ReproCELL), SSEA-4 (diluted at 1:300, MAB4304, CHEMICON), and TRA-1-60 (diluted at 1:300, MAB4360, CHEMICON). Secondary antibodies used were Alexa Fluor 546 Goat Anti-mouse IgG, 2 mg/mL (diluted at 1:300, A11003, Invitrogen), Alexa Fluor 488 Goat Anti-rabbit IgG, 2 mg/mL (diluted at 1:300, A11008, Invitrogen), and Alexa Fluor 488 Goat Anti-mouse IgG, 2 mg/mL, F(ab')2 fragment (diluted at 1:300, A11017, Invitrogen). Nuclei were stained with 1 μg/mL DAPI (40043, Biotium).

Quantitative RT-PCR

RNA was extracted from cells using the RNeasy Plus Mini kit (Qiagen). An aliquot of total RNA was reverse transcribed by using an oligo (dT) primer. For the thermal cycle reactions, the cDNA template was amplified (ABI PRISM 7900HT Sequence Detection System) using the Platinum Quantitative PCR SuperMix-UDG with ROX (11743-100, Invitrogen) under the following reaction conditions: 40 cycles of PCR (95 °C for 15 s and 60 °C for 1 min) after an initial denaturation (95 °C for 2 min). Fluorescence was monitored during every PCR cycle at the annealing step. The authenticity and size of the PCR products were confirmed using a melting curve analysis (using software provided by Applied Biosystems) and a gel analysis. mRNA levels were normalized using *GAPDH* as a housekeeping gene. POU5F1-2-F and POU5F1-3-R primers were used to detect the *OCT4/3* gene (see Table 1, D and F).

Chromatin immunoprecipitation (ChIP) assays

Chromatin immunoprecipitation was performed according to the instructions of the EZ ChIP Chromatin Immunoprecipitation Kit (17-371, Upstate Biotechnology Inc., Chicago, IL, USA). Histone and DNA were cross-linked with 1% formaldehyde for 10 min at room temperature and formaldehyde was then inactivated by the addition of 125 mM glycine. The chromatin was then sonicated to an average DNA fragment length of 200 to 1000 bp. Soluble chromatin reacted with and without anti-acetylated Histone H3 (06-599, Upstate Biotechnology Inc., Chicago, IL, USA), and anti-acetylated Histone H4 (06-866, Upstate Biotechnology Inc., Chicago, IL, USA). The immunocomplex was purified and collected in elution buffer (0.1 M $NaHCO_3$, 1% sodium dodecyl sulfate). Crosslinking was then reversed using elution buffer containing RNase A (0.03 mg/mL) and NaCl (0.3 M) by incubation for 4 h at 65 °C. Supernatant obtained without antibody was used as the input control. The DNA was treated with proteinase K for 1 h at 45 °C and purified. For all ChIP experiments, quantitative PCR analyses were performed in real time as described in this manuscript. Relative occupancy values were calculated by determining the apparent immunoprecipitation efficiency (ratios of the amount of immunoprecipitated DNA to that of the input sample) and normalized to the level observed at a control region. For all the primers used, each gave a single product of the right size adult stem cell confirmed by agarose gel electrophoresis and dissociation curve analysis. These primers also gave no DNA product in the no-template control. The following three primer sets for human *OCT4/3*, as previously described [26], were adopted for real-time PCR to quantitate the ChIP-enriched DNA: human *POU5F1*-A (-2613/-2396), 5′-GGG GAACCTGGAGGATGG-CAAGCTGAGAAA-3′ and 5′-GGCCTGGTGGGGGTGGGAGG AACAT-3′; human *POU5F1*-B (-1779/-1563), 5-CCTGCACCCCTCCACAAATCACTC GC-3′ and 5′-TGCAATCCCCTCAAAGACTGAGCCTCAGAC-3′ ; human *POU5F1*-C (-237/-136), 5′-GAGGGGCGCCAGTTGTGTCTCCCGGTTTT-3′ and 5′-GGGAGGTGGG GGGAGAAACTGAGGCGAAGG-3′.

DNA methylation analysis

The NCR-G2 (JCRB cell bank number; JCRB1167) [32], NCR-G3 (JCRB cell bank number; JCRB1168) [32], GBS6, and Yub636BM (human bone marrow cells derived from an extra digit) cells were prepared for this assay. Genomic DNA was isolated using DNeasy Blood and Tissue Kit (69504, QIAGEN). Primers were selected from the CpG island regions with homogenous CpG site methylation patterns. The target region of the genes used for methylation analysis and the primer sequences used for PCR amplification are shown in Table 4. One of the two primers in the PCR amplification of the target regions is tagged with a T7 promoter sequence: cagtaatacgactcactatagggagaaggct. The PCR reactions were carried out in a total volume of 5 μL using 1 pmol of each primer, 40 μM dNTP, 0.1 U HotStar Taq DNA polymerase (QIAGEN), 1.5 mM $MgCl_2$, 5× PCR buffer (final concentration 1×), and bisulfite-converted DNA. The reaction mix was preactivated for 15 min at 95 °C. The reactions were amplified in 45 cycles of 95 °C for 20 s, 62 °C for 30 s, and 72 °C for 30 s followed by 72 °C for 3 min. Unincorporated dNTPs were dephosphorylated by adding 1.7 μL DNase-free water and 0.3 U Shrimp Alkaline Phosphatase (SAP). The reaction was incubated at 37 °C for 20 min and SAP was then heat-inactivated for 10 min at 85 °C. Typically, 2 μL of the PCR reaction was directly used as a template in a 6.5 μL combined transcription-cleavage reaction. Twenty units of T7 polymerase (Epicentre) were used to incorporate either dCTP or dTTP in the transcripts. Ribonucleotides at 1 mM and the dNTP substrate at 2.5 mM were used. RNase A (Sequenom) was included to cleave the in vitro transcript. The mixture was then further diluted with water to a final volume of 27 μL. Conditioning of the phosphate backbone prior to MALDI-TOF MS was achieved by the addition of 6 mg CLEAN resin (Sequenom). The cleavage reaction samples (15 nL) were dispensed onto silicon

Fig. 3 – In vitro and in vivo characteristics of GBS6 cells. (A) Ca++-dependent, E-cadherin-independent adhesion of GBS6 cell aggregates. GBS6 cells (a) were unaffected by the antibody to E-cadherin (b), but were dissociated by EDTA, Ca++ chelator (c). In contrast, NCR-G3 cells (d), serving as a control since they are E-cadherin-dependent, were dissociated and induced to death by the antibody to E-cadherin (e). Scale bar: 100 μm. (B) Immunohistochemical analysis of GBS6 cells implanted into the subcutaneous tissue of NOG mice. GBS6 cells at 2 weeks after implantation (a, b: hematoxylin and eosin stain, c: silver stain, d: PAS stain) were examined for immunohistochemical analysis using antibodies to MIC2 (e), vimentin (f), neurofilament protein 70 kDa (g: NF-L), desmin (h), and smooth muscle actin (i: SMA). Scale bars: 200 μm (a) and 50 μm (b–i). (C) Immunohistochemical analysis with the anti-OCT4/3 antibody of GBS6 cells implanted into the subcutaneous tissue of NOG mice. GBS6 cells at 2 weeks after implantation were examined for immunohistochemical analysis using antibodies to OCT4/3. The higher-magnification image of the region enclosed by a square in "a" (b). Scale bars: 200 μm (a) and 20 μm (b).

chips preloaded with matrix (SpectroCHIP, Sequenom). Mass spectra were collected using a MassARRAY mass spectrometer (Sequenom). Spectra were analyzed using proprietary peak picking and spectra interpretation tools (EpiTYPER, Sequenom).

For analysis of DNA methylation, we examined the methylation-dependent C/T sequence changes introduced by bisulfite treatment. Those C/T changes are reflected as G/A changes on the reverse strand and hence result in a mass difference of 16 kDa for

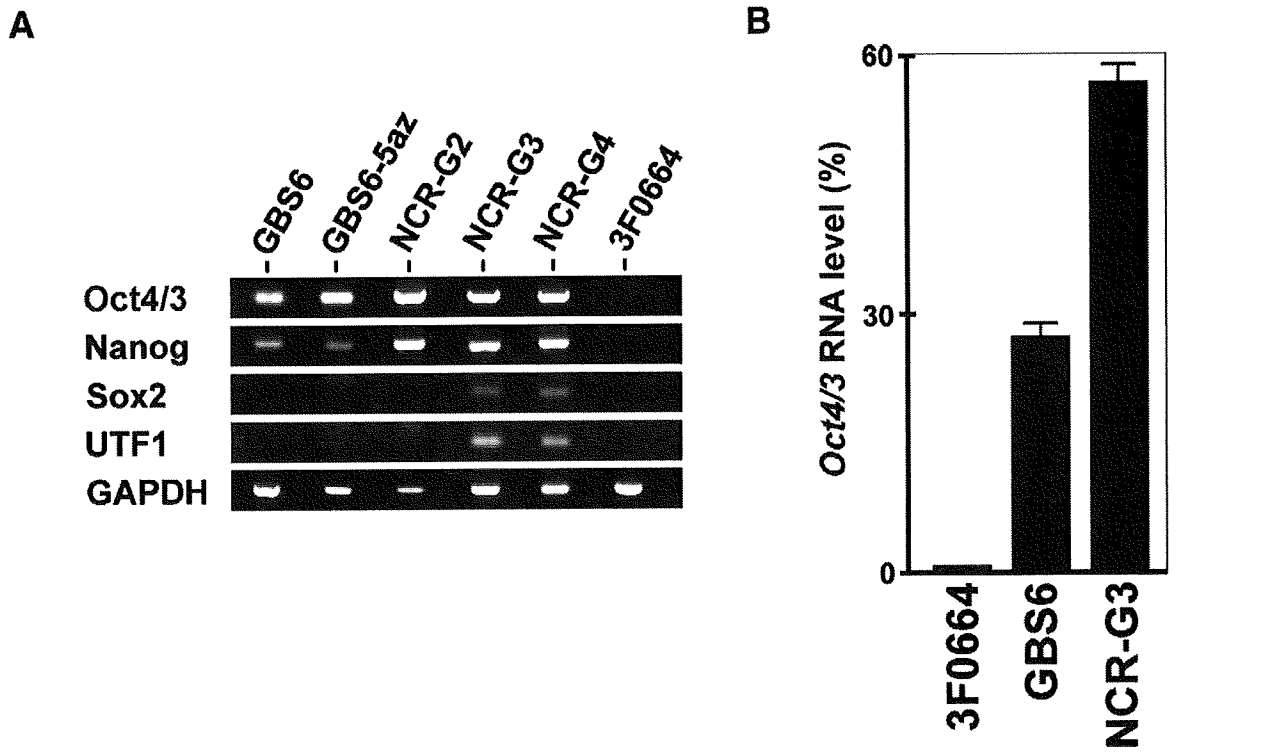

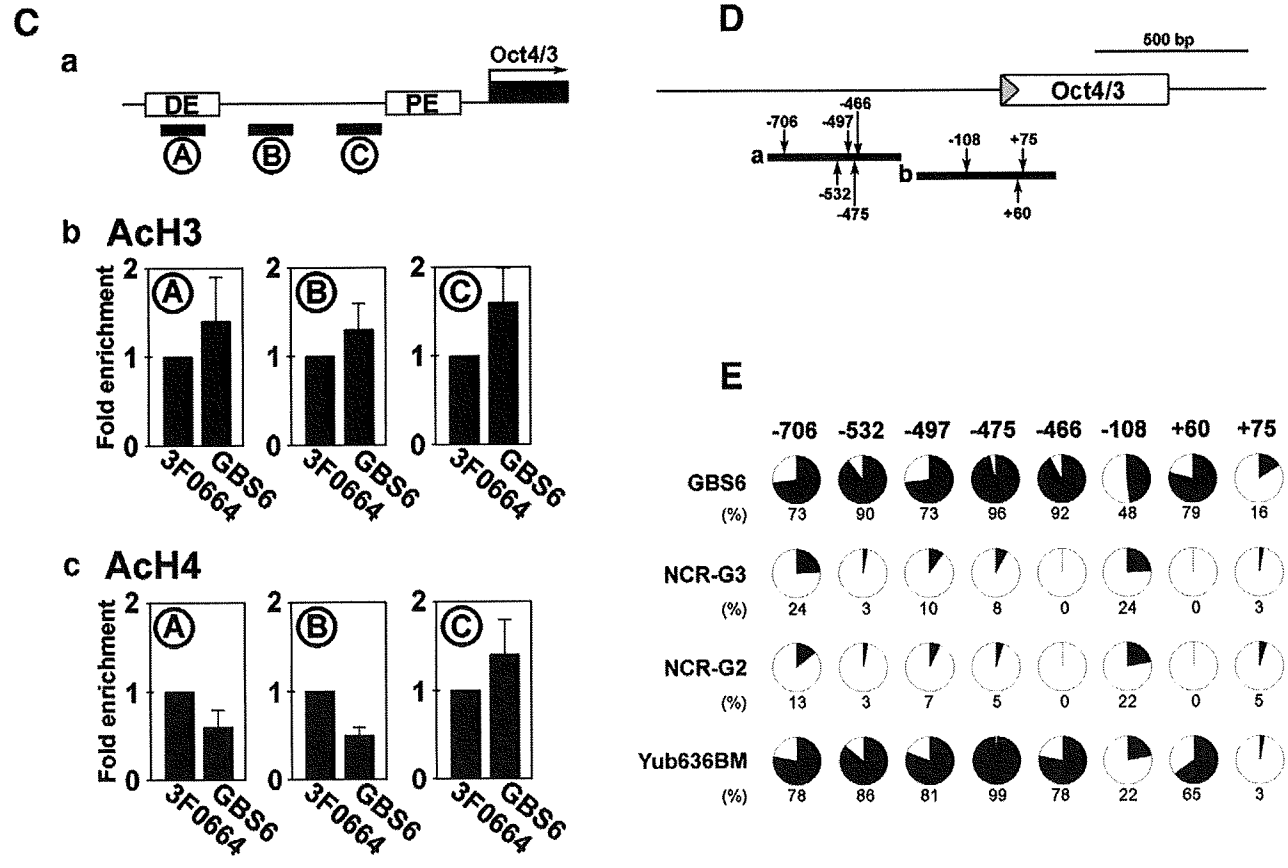

each CpG site enclosed in the cleavage products generated from the RNA transcript. The mass signals representing nonmethylated DNA and those representing methylated DNA, built signal pairs, which are representative for the CpG sites within the analyzed sequence substring. The intensities of the peaks were compared, and the relative amount of methylated DNA was calculated from this ratio. The method yields quantitative results for each of these sequence-defined analytic units referred to as CpG units, which contain either one individual CpG site or an aggregate of subsequent CpG sites.

Plasmid construction

Each open reading frame of human *OCT4/3* and *SOX2* was amplified by RT-PCR using the RNA extracted from NCR-G2 cells (JCRB cell bank number; JCRB1167) [32], a complex-type germ cell tumor cell line. Also, those of *c-MYC* and *KLF4* were amplified by RT-PCR using the RNA extracted from the bone marrow stromal cell line, UET13. A Gateway cassette composed of an attR1/R2 flanked CmR and ccdB (Invitrogen) was amplified by PCR and ligated into the Eco RI/Not I site of pMXs retroviral expression vector to create pMXs-DEST [37]. PCR amplification was performed by using KOD-Plus-DNA polymerase (KOD-201, TOYOBO). The constructs were confirmed by sequencing.

Retroviral infection and iPS cell generation

293FT cells (Invitrogen) were plated at 2×10^6 cells per 100 mm dish and incubated overnight. The next day, the cells were co-transfected with pMXs-OCT4/3, pMXs-SOX2, pMXs-c-MYC, pMXs-KLF4, pCL-GagPol, and pHCMV-VSV-G vectors with TransIT-293 reagent (Mirus, Madison, WI). Twenty-four hours after transfection, the medium was replaced with a new medium, which was collected after 48 h as the virus-containing supernatant. MRC-5 cells were seeded at 1×10^5 cells per 35 mm dish 1 day before infection. The virus-containing supernatants were filtered through a 0.45 μm pore-size filter, ultracentrifuged at 8500 rpm for 16 h, and then resuspended in DMEM (D6429, SIGMA) supplemented with 4 mg/mL polybrene (Nacalai Tesque). Equal amounts of concentrated supernatants containing each of the four retroviruses were mixed, transferred to MRC-5 cells, and incubated for 8 h. The MRC-5 cells were cultured for 4 days and replated on an irradiated MEF feeder layer in 100 mm dish. The medium was replaced with the iPSellon medium supplemented with 10 ng/mL bFGF. One-half of the medium was changed every day and the cells were cultured up to 30 days after a day of infection. Colonies were picked up and transferred into 0.2 mL of iPSellon medium when colonies appeared. The colonies were mechanically dissociated to small clumps by pipeting up and down or mechanically cut using a STEMPRO EZPassage disposable passaging tool (23181010, Invitrogen). The cell suspension was transferred on irradiated MEF feeder in 4-well plates [176740, Nunc (Thermo Fisher Scientific)]. We define this stage as passage 1.

Teratoma formation

iPS cells were harvested by accutase treatment, collected into tubes, and centrifuged, and the pellets were suspended in the iPSellon medium. The same volume of Basement Membrane Matrix (354234, BD Biosciences) was added to the cell suspension. Cells (1×10^7) were implanted subcutaneously to a BALB/c-*nu/nu* mouse (CREA, Japan) for 4 weeks. Tumors were dissected and fixed with PBS containing 4% paraformaldehyde. Paraffin-embedded tissue was sliced and stained with hematoxylin and eosin.

GeneChip expression analysis

Total RNA was extracted from cells using the RNeasy Mini Kit (74104, Qiagen, Valencia, CA). Genomic DNA was eliminated by DNase I (2215A, TAKARA BIO INC.) treatments. From all RNA samples, 5 μg of total RNA was used as a starting material for the microarray sample preparation. Double-stranded cDNA was synthesized from DNase-treated total RNA, and the cDNA was subjected to in vitro transcription in the presence of biotinylated nucleoside triphosphates using the Enzo BioArray HighYield RNA Transcript Labeling Kit (Enzo Life Sciences, Inc., Farmingdale, NY), according to the manufacturer's protocol (One-Cycle Target Labeling and Control Reagent package). Human-genome-wide gene expression was examined with the Human Genome U133A Probe array (GeneChip, Affymetrix), which contains the oligonucleotide probe set for approximately 23,000 full-length genes and expressed sequence tags (ESTs), according to the manufacturer's protocol (Expression Analysis Technical Manual and GeneChip small sample target labeling Assay Version 2 technical note, http://www.affymetrix.com/support/technical/index.affx) as previously described [5]. Hierarchical clustering and principle component

Fig. 4 – Expression of the *OCT4/3* gene and histone modification of the *OCT4/3* promoter in GBS6 cells. (A) Expression of embryonic stem cell-enriched genes in GBS6, NCR-G2, NCR-G3, NCR-G4, and 3F0664 cells. GBS6 cells expressed the *OCT4/3* and *NANOG* genes, but not the *SOX2* and *UTF1* genes. NCR-G2 cells expressed the *OCT4/3* and *NANOG* genes; both NCR-G3 cells and NCR-G4 cells expressed the *OCT4/3*, *NANOG*, *SOX2* and *UTF1* genes. 3F0664 mesenchymal cells did not express these four kinds of embryonic stem cell-enriched genes. POU5F1-1a-F and POU5F1-1a-R (Table 1) were used to amplify the endogenous *OCT4/3* gene. (B) Quantitative PCR analysis to assess the expression level of *OCT4/3* mRNA in GBS6. *OCT4/3* mRNA level is expressed relative to 3F0664 cells control. (C) Real-time PCR to quantitate the ChIP-enriched DNA using acetylated Histone H3 and acetylated Histone H4 antibodies. Schematic of the location of the amplicons (A–C) used to detect ChIP-enriched fragments in *OCT4/3* shown relative to the distal enhancer (DE)/CR4 region, to the proximal enhancer (PE), and to transcription start site (arrow) (a). The relative levels of acetylated Histone H3 (b) and acetylated Histone H4 (c) modifications were detected in GBS6 cells and 3F0664 cell control. GBS6 cells are represented by black bars and 3F0664 cells by open bars. (D) DNA methylation analysis in the promoter region of the *OCT4/3* gene. The target regions of *OCT4/3* used for the quantitative DNA methylation analysis. Region 'a' and Region 'b' include 5 (−706, −532, −497, −475, −466) and 3 (−108, +60, +75) CpG sites, respectively. The positions of CpG sites are relative to the *OCT4/3* transcription start site (gray triangle). (E) The relative amount of methylated DNA ratio (%) at each CpG site is indicated as the black area in the pie chart.

analysis were performed to group mesenchymal cells obtained from bone marrow into subcategories (http://lgsun.grc.nia.nih.gov/ANOVA/).

Results

Establishment of human cells of mesenchymal origin with overexpression of the translocated POU5F1/OCT4/3 gene

To investigate whether cells of mesenchymal origin acquire an embryonic phenotype, a novel human cell line termed GBS6 was established from the pelvic bone tumor, of which histology shows diffuse proliferation of undifferentiated tumor cells with oval nuclei and scant but short spindle cytoplasm [31]. The generated cells grew attached to the dish as a polygonal cell sheet with cell aggregates forming in the center (Figs. 1A, B), and retained the reciprocal translocation, t(6; 22), detected in the original tumor (Fig. 1C). The *EWS-OCT4/3* chimeric gene expression also remained (Figs. 1D, E and Table 1). Embryonal carcinoma (EC) cells, i.e., NCR-G2, NCR-G3, and NCR-G4, served as control cells expressing the endogenous *OCT4/3* gene. Immunoblot analysis revealed that EWS-OCT4/3 fusion protein was expressed in GBS6 cells (Fig. 1F).

Cell surface markers of GBS6 cells

GBS6 cell surface markers were evaluated by flow cytometric analysis (Fig. 2). The results showed that GBS6 cells were strongly positive (Positive; Fig. 2B) for CD9, CD29 (integrin β1), CD44, CD59, CD81, CD90 (Thy-1) and HLA-A,B,C (HLA class I); weakly positive (Low; Fig. 2B) for CD73 and CD166 (ALCAM); negative (Negative; Fig. 2B) for CD55, CD105 (endogrin), CD140a (PDGFRα), and CD140b (PDGFRβ). The lack of CD13, CD55, CD105, CD106, CD140a, and CD140b in GBS6 cells suggests that the surface markers of GBS6 cells are different from those of conventional mesenchymal cells [10,38,39].

E-cadherin-independent growth of GBS6 cells

To investigate whether GBS6 cells survive dependent on E-cadherin-like human embryonic cells, the cells were treated by an inhibitory antibody to E-cadherin (HECD Ab) and EDTA (Fig. 3A). GBS6 cell survival was unaffected by the E-cadherin antibody but affected by EDTA (Fig. 3A-a, b, c). In contrast, NCR-G3 cells, human embryonal carcinoma cells that proliferate in an E-cadherin-dependent manner, were dissociated and induced to apoptosis by the E-cadherin antibody (Fig. 3A-d, e).

Implantation of GBS6 cells into immunodeficient mice

To investigate an in vivo phenotype of GBS6 cells, the cells were intramuscularly injected into immunodeficient NOG mice and examined by histopathology and immunohistochemistry (Fig. 3B). The injected cells exhibited an undifferentiated phenotype with oval nuclei and scant spindle cytoplasm (Fig. 3B-b), and showed an alveolar configuration (Fig. 3B-c). The cells were negative by the PAS stain (Fig. 3B-d). The cells were immunohistochemically positive for MIC2 and vimentin (Fig. 3B-e, f), and negative for neurofilament, desmin, and smooth muscle actin (Fig. 3B-g, h, i). The cells retained OCT4/3 in their nuclei even after implantation (Fig. 3C).

Expression of ES-enriched genes

To determine if GBS6 cells express ES cell-enriched genes, that is, the *OCT4/3*, *NANOG*, *SOX2*, and *UTF1* genes, RT-PCR with specific primer sets (Table 2) and gene chip analyses were performed. GBS6 cells expressed the endogenous *OCT4/3* and *NANOG* genes like NCR-G2, NCR-G3, and NCR-G4 embryonal carcinoma cells, but did not express the *SOX2* and *UTF1* genes (Fig. 4A). The results of the RT-PCR analysis were compatible with those of the gene chip analysis (GSE8113, Table 3). To compare the expression level of stem cell-specific genes in GBS6 cells, ES cells, and mesenchymal cells, we performed a quantitative RT-PCR analysis. The expression level of *OCT4/3* was about half that of human EC cells, but was more than twenty-five times that of 3F0664 mesenchymal cells (Fig. 4B). The results show that the expression level of *OCT4/3* is comparable to that of human EC cell.

To determine if the cis-regulatory element of the *OCT4/3* gene has so-called open chromatin structure, we performed the chip analysis using antibodies to acetylated H3 and acetylated H4 (Fig. 4C). The results show that acetylated histone levels which the *OCT4/3* promoter is wrapped around in GBS6 cells are comparable with those in 3F0664 mesenchymal cells. We also performed methylation analysis of the *OCT4/3* gene in GBS6 cells because the expression of *OCT4/3* gene is regulated by methylation (Figs. 4D, E and Table 4). The promoter region of the *OCT4/3* gene was heavily methylated in GBS6 cells as compared with human NCR-G3 embryonal carcinoma cells expressing the *OCT4/3* gene at a high level.

Cell reprogramming assay

To investigate if chimeric EWS-OCT4/3 induces iPS cells like native OCT4/3, we performed Yamanaka's reprogramming assay on MRC-5 human fetal lung fibroblasts (Fig. 5A), using the chimeric *EWS-OCT4/3* construct with the *KLF-4*, *SOX2*, and *c-MYC* genes according to the conventional protocol [40] with some modifications. We failed to obtain iPS cells using the *EWS-OCT4/3*, *KLF-4*, *SOX2*, and *c-MYC* constructs (Fig. 5B), albeit trials of three independent experiments, whereas, for a control, we successfully generated 101 clones of iPS cells from MRC-5 cells using the *OCT4/3*, *KLF-4*, *SOX2*, and *c-MYC* constructs (Fig. 5C). The iPS cells generated from MRC-5 cells expressed human ES cell-specific surface antigens (Figs. 5D–G). In vivo implantation analysis showed that iPS cells generated various tissues including neural tissues (Fig. 5H: ectoderm), cartilage (Fig. 5I: mesoderm),

Table 4 – Primers used for PCR amplification of the bisulfite-converted DNA.

Name	Sequence	Size (bp)
Region 'a'	Forward: 5′ TTG GTT ATT GTG TTT ATG GTT GTT G 3′	437
	Reverse: 5′ TAA ACC AAA ACA ATC CTT CTA CTC C 3′	
Region 'b'	Forward: 5′ TTT GGG TAA TAA AGT GAG ATT TTG TTT 3′	452
	Reverse: 5′ CTA ACC CTC CAA AAA AAC CTT AAA A 3′	

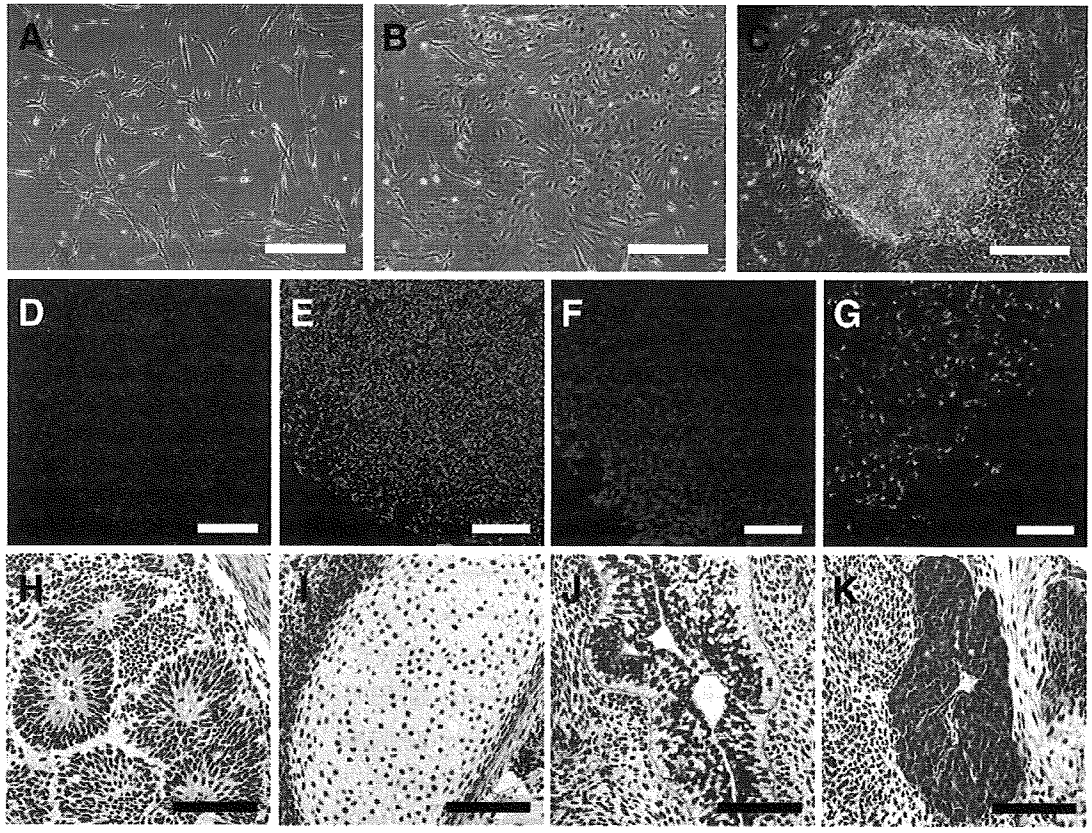

Fig. 5 – Induction of iPS cells from MRC-5 cells and teratoma formation. (A) Morphology of MRC-5 cells. (B) Morphology of cells using *EWS-OCT4/3*, *KLF-4*, *SOX2*, and *c-MYC* genes at Day 30 after infection. (C) Morphology of established iPS cell (clone 16: Fetch) colony using *OCT4/3*, *KLF-4*, *SOX2*, and *c-MYC* genes at Day 20 after infection. (D–G) Immunocytochemistry for OCT4/3 (D), NANOG (E), SSEA-4 (F), and TRA-1-60 (G). Nuclei were stained with DAPI. Bars = 500 μm (A–C), and 200 μm (D–G). In addition, chromosomal G-band analyses showed that human iPS cells from MRC-5 had a normal karyotype of 46XY (not shown). The analysis of short tandem repeat shows that novel iPS cells from MRC-5 cells were not a result of cross-contamination. Hematoxylin and eosin staining of teratoma derived from the generated iPS cells. Cells (1×10^7) were implanted subcutaneously to a BALB/c-*nu/nu* mouse for 4 weeks. Histological examination showed that the tumor contained various tissues, neural tissues (H; ectoderm), cartilage (I; mesoderm), a gut-like epithelial tissue (J; endoderm), and a hepatic tissue (K; endoderm). Bars = 100 μm (H–K).

a gut-like epithelial tissue (Fig. 5J: endoderm), and a hepatic tissue (Fig. 5K: endoderm). These results imply that the chimeric *EWS-OCT4/3* gene does not participate in reprogramming of somatic cells.

Principle component analysis of global gene expression in GBS6 cells

To determine whether GBS6 cells are categorized into embryonal cells or mesenchymal cells, global gene expression patterns of GBS6 cells, embryonal carcinoma cells (NCR-G2, NCR-G3, and NCR-G4), yolk sac tumor cells (NCR-G1), and marrow stromal cells (3F0664, H4-1, and Yub10F) were further analyzed by principle component analysis (PCA), which reduces high-dimensionality data into a limited number of principle components (Fig. 6). The first principle component (PC1) captures the largest contributing factor of variation, which characterizes the differential expression of genes. As we were interested in the differential gene expression component, we plotted the position of each cell type against the PC1, PC2, and PC3 axis in three-dimensional space by using virtual reality modeling language (Fig. 6A). Close examination of the 3D model identified PC1 as the most representative view of the 3D model. PC1 axis direction is therefore used to characterize the differential gene expression (Fig. 6B). In addition, hierarchical analysis of the cells analyzed for global gene expression revealed that GBS6 cells are categorized into embryonal carcinoma cells and yolk sac tumor cells, i.e., NCR-G1, -G2, -G3, and -G4 cells (Fig. 6C).

Discussion

In this study, we generated a cell line with a transitional form between mesenchymal cells and embryonic stem cells. Loss of mesenchyme-specific cell markers, i.e., CD13, CD55, CD105, CD106, CD140a and CD140b, and modification of cell survival with the calcium chelator indicate that GBS6 cells are no longer mesenchymal cells. Global and drastic differences in gene expression with the GeneChip analysis support the conclusion that GBS6 cells no longer exhibit the profile of mesenchymal cells. It is also noteworthy that this transition phenotype is reliably inherited ex vivo after a series of in vitro passages.

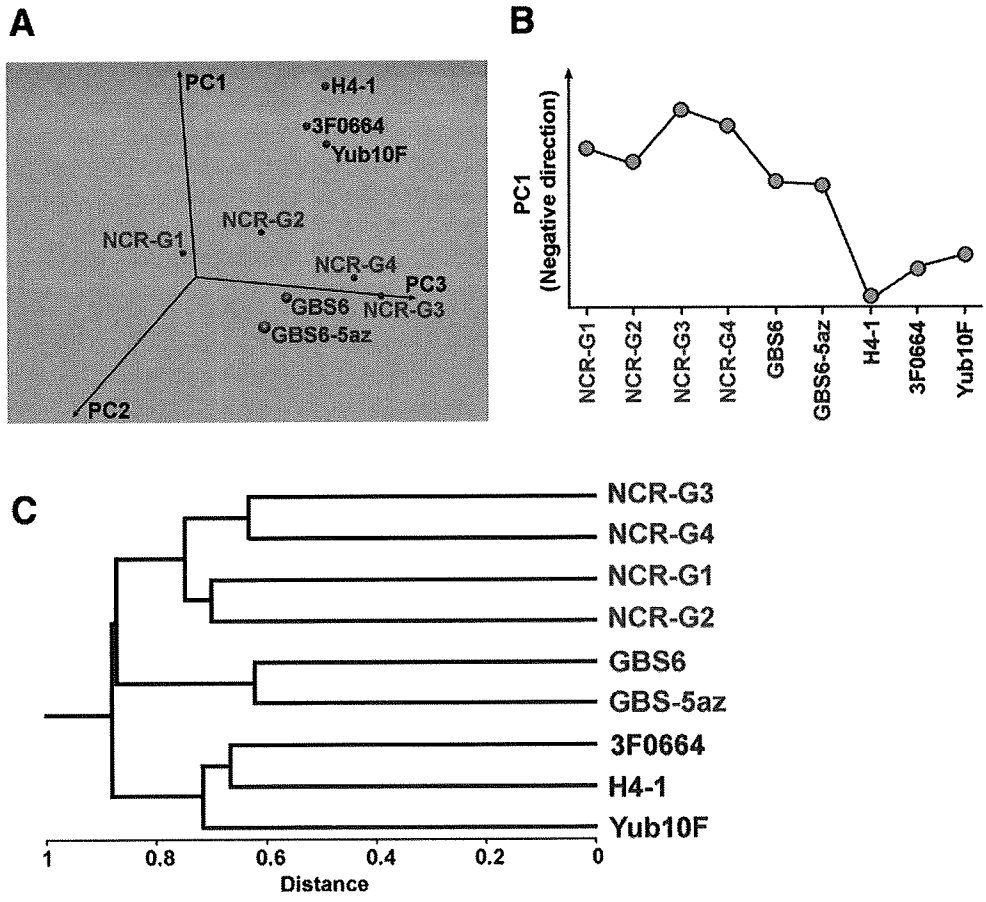

Fig. 6 – Principal component analysis and hierarchical clustering of gene expression in GBS6 cells, embryonal carcinoma cells, and bone marrow cells. (A) 3D-representation of principle component analysis. (B) Principal components of PC1 axis, negative direction. (C) Hierarchical clustering analysis of averages.

OCT4/3 function and its physiological partner EWS in embryonic transition

ES-like cells or iPS cells are generated from murine fibroblasts by transfecting four genes, i.e., *OCT4/3*, *SOX2*, *KLF-4* and *c-MYC* are necessary for the mesenchymal–embryonic transition [1–3]. However, OCT4/3 alone is not sufficient to confer embryonic phenotypes to human bone marrow-derived cells, NIH3T3 cells (data not shown) or embryonic fibroblasts [1]. EWS and OCT4/3 are directly bound both in vitro and in vivo [41]; in other words, EWS is a binding partner of OCT4/3. Therefore, the EWS-OCT4/3 protein in GBS6 cells is considered a fusion between physiological partners. EWS and OCT4/3 are co-expressed in the pluripotent mouse and human ES cells. To investigate if the EWS-OCT4/3 has a transcriptional activity, we performed the luciferase assay. The results show that the chimeric *EWS-OCT4/3* gene has comparable or higher transcriptional activity than the native *OCT4/3* gene does (Supplementary Fig. S1). Ectopic expression of non-chimeric EWS enhances the transactivation activity of OCT4/3; the N-terminal QSY domain of EWS and the C-terminal POU domain function as a transcriptional activation and DNA binding, respectively [42,43]. The *OCT4/3* gene is overexpressed under the cis-regulatory element of the *EWS* gene [31], and the functional co-operation of OCT4/3 and EWS at a protein level to transcriptional activation may lead to embryonic transformation in GBS6 cells. Converting mesenchymal cells to embryonic cells opposes the usual direction of ES cell differentiation [44]; and this is achieved by chimeric OCT4/3 with physiological co-activator EWS driven by the potent cis-regulatory element of the *EWS* gene [31]. This phenotypic conversion requires the molecular reprogramming of mesenchymal cells with new instructions.

Mesenchymal to embryonic "incomplete" transition by overexpression of chimeric OCT4/3

OCT4/3 fused to *EWS* not only participates in oncogenesis [29,31], but also contributes to mesenchymal–embryonic transition, at least in part from the viewpoint of global gene expression profiles and cell surface markers (Figs. 2 and 6). GBS6 cells are subcategorized into groups of cells derived from testicular germ cell tumors (Fig. 6A, cells with embryonic phenotypes are shown in pink), and the PC1 axis indicates transition from mesenchymal cell group to embryonal cell group (Fig. 6B). This transition was, however, incomplete; some of the ES-specific genes were not reactivated. OCT4/3 is a member of the POU family of transcription factors, is expressed in pluripotent ES cells, including primordial germ cells [17–21], and functions as a master switch in differentiation by regulating cells that have, or can develop, pluripotent

potential. However, tight chromatin structure in GBS6 cells may render OCT4/3 recognition sequences inaccessible [45]. The OCT4/3 recognition sequences have been found in the cis-regulatory elements of the FGF-4 and CD140a/platelet-derived growth factor receptor-α gene [46], but GBS6 cells are indeed negative for CD140a (Fig. 2B). Alternatively, the lack of other essential transcription factors such as SOX2 and UTF1 (Fig. 4A, Table 3) and/or co-factors may be a cause of "incomplete" transition. Interestingly, this transition phenotype is reliably inherited ex vivo after a series of in vitro passages, and this may also be attributed to the function of OCT4/3 that is critical for self-renewal of embryonic stem cells [24].

Mesenchymal to epithelial transition is observed in physiological and pathological conditions [47–50]. In contrast, mesenchymal–embryonic transition has been achieved in an artificial experimental condition in vitro [1–3]. Homogenous positive staining for OCT4/3 in embryonal carcinoma cells supports the model that the encoded protein is crucial, and the absence of OCT4/3 in non-embryonal carcinoma cells is in agreement with the inability to generate pluripotent stem cells [51]. The cell line generated in this study with overexpression of chimeric OCT4/3, although this is just one case of rare human immortalized cells, provides us with insight into cell plasticity involving OCT4/3 that is essential for ES cell maintenance and into the complexity required for changing cellular identity.

Acknowledgments

We would like to express our sincere thanks to Michiyo Nasu for histological analysis, Yoriko Takahashi for data mining, and Kayoko Saito for secretary work. This study was supported by grants from the Ministry of Education, Culture, Sports, Science and Technology (MEXT) of Japan and Health and Labor Sciences Research Grants; by Research on Health Science Focusing on Drug Innovation from the Japan Health Science Foundation; by the Program for Promotion of Fundamental Studies in Health Science of the Pharmaceuticals and Medical Devices Agency; by the grant from Terumo Life Science Foundation; by a research Grant for Cardiovascular Disease from the Ministry of Health, Labor and Welfare; and by a Grant for Child Health and Development from the Ministry of Health, Labor and Welfare.

Appendix A. Supplementary data

Supplementary data associated with this article can be found, in the online version, at doi:10.1016/j.yexcr.2009.06.016.

REFERENCES

[1] K. Takahashi, S. Yamanaka, Induction of pluripotent stem cells from mouse embryonic and adult fibroblast cultures by defined factors, Cell 126 (2006) 663–676.
[2] K. Okita, T. Ichisaka, S. Yamanaka, Generation of germline-competent induced pluripotent stem cells, Nature 448 (2007) 313–317.
[3] M. Wernig, A. Meissner, R. Foreman, T. Brambrink, M. Ku, K. Hochedlinger, B.E. Bernstein, R. Jaenisch, In vitro reprogramming of fibroblasts into a pluripotent ES-cell-like state, Nature 448 (2007) 318–324.
[4] M.J. Go, C. Takenaka, H. Ohgushi, Forced expression of Sox2 or Nanog in human bone marrow derived mesenchymal stem cells maintains their expansion and differentiation capabilities, Exp. Cell Res. 314 (2008) 1147–1154.
[5] T. Mori, T. Kiyono, H. Imabayashi, Y. Takeda, K. Tsuchiya, S. Miyoshi, H. Makino, K. Matsumoto, H. Saito, S. Ogawa, M. Sakamoto, J. Hata, A. Umezawa, Combination of hTERT and bmi-1, E6, or E7 induces prolongation of the life span of bone marrow stromal cells from an elderly donor without affecting their neurogenic potential, Mol. Cell. Biol. 25 (2005) 5183–5195.
[6] R.H. Lee, B. Kim, I. Choi, H. Kim, H.S. Choi, K. Suh, Y.C. Bae, J.S. Jung, Characterization and expression analysis of mesenchymal stem cells from human bone marrow and adipose tissue, Cell. Physiol. Biochem. 14 (2004) 311–324.
[7] J.G. Toma, M. Akhavan, K.J. Fernandes, F. Barnabe-Heider, A. Sadikot, D.R. Kaplan, F.D. Miller, Isolation of multipotent adult stem cells from the dermis of mammalian skin, Nat. Cell Biol. 3 (2001) 778–784.
[8] C.H. Cui, T. Uyama, K. Miyado, M. Terai, S. Kyo, T. Kiyono, A. Umezawa, Menstrual blood-derived cells confer human dystrophin expression in the murine model of duchenne muscular dystrophy via cell fusion and myogenic transdifferentiation, Mol. Biol. Cell 18 (2007) 1586–1594.
[9] O.K. Lee, T.K. Kuo, W.M. Chen, K.D. Lee, S.L. Hsieh, T.H. Chen, Isolation of multipotent mesenchymal stem cells from umbilical cord blood, Blood 103 (2004) 1669–1675.
[10] M. Terai, T. Uyama, T. Sugiki, X.K. Li, A. Umezawa, T. Kiyono, Immortalization of human fetal cells: the life span of umbilical cord blood-derived cells can be prolonged without manipulating p16INK4a/RB braking pathway, Mol. Biol. Cell 16 (2005) 1491–1499.
[11] X. Zhang, A. Mitsuru, K. Igura, K. Takahashi, S. Ichinose, S. Yamaguchi, T.A. Takahashi, Mesenchymal progenitor cells derived from chorionic villi of human placenta for cartilage tissue engineering, Biochem. Biophys. Res. Commun. 340 (2006) 944–952.
[12] E.H. Allan, P.W. Ho, A. Umezawa, J. Hata, F. Makishima, M.T. Gillespie, T.J. Martin, Differentiation potential of a mouse bone marrow stromal cell line, J. Cell. Biochem. 90 (2003) 158–169.
[13] H. Imabayashi, T. Mori, S. Gojo, T. Kiyono, T. Sugiyama, R. Irie, T. Isogai, J. Hata, Y. Toyama, A. Umezawa, Redifferentiation of dedifferentiated chondrocytes and chondrogenesis of human bone marrow stromal cells via chondrosphere formation with expression profiling by large-scale cDNA analysis, Exp. Cell Res. 288 (2003) 35–50.
[14] S. Makino, K. Fukuda, S. Miyoshi, F. Konishi, H. Kodama, J. Pan, M. Sano, T. Takahashi, S. Hori, H. Abe, J. Hata, A. Umezawa, S. Ogawa, Cardiomyocytes can be generated from marrow stromal cells in vitro, J. Clin. Invest. 103 (1999) 697–705.
[15] N. Nishiyama, S. Miyoshi, N.M. Hida, T. Uyama, K. Okamoto, Y. Ikegami, K. Miyado, K. Segawa, M. Terai, M. Sakamoto, S. Ogawa, A. Umezawa, The significant cardiomyogenic potential of human umbilical cord blood-derived mesenchymal stem cells in vitro, Stem Cells 25 (2007) 2017–2024.
[16] J. Deng, B.E. Petersen, D.A. Steindler, M.L. Jorgensen, E.D. Laywell, Mesenchymal stem cells spontaneously express neural proteins in culture and are neurogenic after transplantation, Stem Cells 24 (2006) 1054–1064.
[17] H.R. Scholer, G.R. Dressler, R. Balling, H. Rohdewohld, P. Gruss, Oct-4: a germline-specific transcription factor mapping to the mouse t-complex, EMBO J. 9 (1990) 2185–2195.
[18] K. Okamoto, H. Okazawa, A. Okuda, M. Sakai, M. Muramatsu, H. Hamada, A novel octamer binding transcription factor is differentially expressed in mouse embryonic cells, Cell 60 (1990) 461–472.
[19] M.H. Rosner, M.A. Vigano, K. Ozato, P.M. Timmons, F. Poirier, P.W. Rigby, L.M. Staudt, A POU-domain transcription factor in early

stem cells and germ cells of the mammalian embryo, Nature 345 (1990) 686-692.
[20] M.F. Pera, D. Herszfeld, Differentiation of human pluripotent teratocarcinoma stem cells induced by bone morphogenetic protein-2, Reprod. Fertil. Dev. 10 (1998) 551-555.
[21] T. Goto, J. Adjaye, C.H. Rodeck, M. Monk, Identification of genes expressed in human primordial germ cells at the time of entry of the female germ line into meiosis, Mol. Hum. Reprod. 5 (1999) 851-860.
[22] M. Pesce, X. Wang, D.J. Wolgemuth, H. Scholer, Differential expression of the Oct-4 transcription factor during mouse germ cell differentiation, Mech. Dev. 71 (1998) 89-98.
[23] J. Nichols, B. Zevnik, K. Anastassiadis, H. Niwa, D. Klewe-Nebenius, I. Chambers, H. Scholer, A. Smith, Formation of pluripotent stem cells in the mammalian embryo depends on the POU transcription factor Oct4, Cell 95 (1998) 379-391.
[24] H. Niwa, J. Miyazaki, A.G. Smith, Quantitative expression of Oct-3/4 defines differentiation, dedifferentiation or self-renewal of ES cells, Nat. Genet. 24 (2000) 372-376.
[25] B. Abdel-Rahman, M. Fiddler, D. Rappolee, E. Pergament, Expression of transcription regulating genes in human preimplantation embryos, Hum. Reprod. 10 (1995) 2787-2792.
[26] J.L. Chew, Y.H. Loh, W. Zhang, X. Chen, W.L. Tam, L.S. Yeap, P. Li, Y.S. Ang, B. Lim, P. Robson, H.H. Ng, Reciprocal transcriptional regulation of Pou5f1 and Sox2 via the Oct4/Sox2 complex in embryonic stem cells, Mol. Cell. Biol. 25 (2005) 6031-6046.
[27] O. Delattre, J. Zucman, B. Plougastel, C. Desmaze, T. Melot, M. Peter, H. Kovar, I. Joubert, P. de Jong, G. Rouleau, A. Aurias, G. Thomas, Gene fusion with an ETS DNA-binding domain caused by chromosome translocation in human tumours, Nature 359 (1992) 162-165.
[28] F. Urano, A. Umezawa, W. Hong, H. Kikuchi, J. Hata, A novel chimera gene between EWS and E1A-F, encoding the adenovirus E1A enhancer-binding protein, in extraosseous Ewing's sarcoma, Biochem. Biophys. Res. Commun. 219 (1996) 608-612.
[29] F. Mitelman, B. Johansson, F. Mertens, The impact of translocations and gene fusions on cancer causation, Nat. Rev. Cancer 7 (2007) 233-245.
[30] M. Kuroda, T. Ishida, M. Takanashi, M. Satoh, R. Machinami, T. Watanabe, Oncogenic transformation and inhibition of adipocytic conversion of preadipocytes by TLS/FUS-CHOP type II chimeric protein, Am. J. Pathol. 151 (1997) 735-744.
[31] S. Yamaguchi, Y. Yamazaki, Y. Ishikawa, N. Kawaguchi, H. Mukai, T. Nakamura, EWSR1 is fused to POU5F1 in a bone tumor with translocation t(6;22)(p21;q12), Genes Chromosomes Cancer 43 (2005) 217-222.
[32] J. Hata, J. Fujimoto, E. Ishii, A. Umezawa, Y. Kokai, Y. Matsubayashi, H. Abe, S. Kusakari, H. Kikuchi, T. Yamada, T. Maruyama, Differentiation of human germ cell tumor cells in vivo and in vitro. Acta Histochem. Cytochem. 25 (1992) 563-576.
[33] E. Schrock, T. Veldman, H. Padilla-Nash, Y. Ning, J. Spurbeck, S. Jalal, L.G. Shaffer, P. Papenhausen, C. Kozma, M.C. Phelan, E. Kjeldsen, S.A. Schonberg, P. O'Brien, L. Biesecker, S. du Manoir, T. Ried, Spectral karyotyping refines cytogenetic diagnostics of constitutional chromosomal abnormalities, Hum. Genet. 101 (1997) 255-262.
[34] M. Sano, A. Umezawa, H. Abe, A. Akatsuka, S. Nonaka, H. Shimizu, M. Fukuma, J. Hata, EAT/mcl-1 expression in the human embryonal carcinoma cells undergoing differentiation or apoptosis, Exp. Cell Res. 266 (2001) 114-125.
[35] S. Gojo, N. Gojo, Y. Takeda, T. Mori, H. Abe, S. Kyo, J. Hata, A. Umezawa, In vivo cardiovasculogenesis by direct injection of isolated adult mesenchymal stem cells, Exp. Cell Res. 288 (2003) 51-59.
[36] T. Sugimoto, A. Umezawa, J. Hata, Neurogenic potential of Ewing's sarcoma cells, Virchows Arch. 430 (1997) 41-46.
[37] Y. Miyagawa, H. Okita, H. Nakaijima, Y. Horiuchi, B. Sato, T. Taguchi, M. Toyoda, Y.U. Katagiri, J. Fujimoto, J. Hata, A. Umezawa, N. Kiyokawa, Inducible expression of chimeric EWS/ETS proteins confers Ewing's family tumor-like phenotypes to human mesenchymal progenitor cells, Mol. Cell. Biol. 28 (2008) 2125-2137.
[38] B.L. Yen, H.I. Huang, C.C. Chien, H.Y. Jui, B.S. Ko, M. Yao, C.T. Shun, M.L. Yen, M.C. Lee, Y.C. Chen, Isolation of multipotent cells from human term placenta, Stem Cells 23 (2005) 3-9.
[39] E.K. Waller, J. Olweus, F. Lund-Johansen, S. Huang, M. Nguyen, G.R. Guo, L. Terstappen, The "common stem cell" hypothesis reevaluated: human fetal bone marrow contains separate populations of hematopoietic and stromal progenitors, Blood 85 (1995) 2422-2435.
[40] K. Takahashi, K. Tanabe, M. Ohnuki, M. Narita, T. Ichisaka, K. Tomoda, S. Yamanaka, Induction of pluripotent stem cells from adult human fibroblasts by defined factors, Cell 131 (2007) 861-872.
[41] J. Lee, B.K. Rhee, G.Y. Bae, Y.M. Han, J. Kim, Stimulation of Oct-4 activity by Ewing's sarcoma protein, Stem Cells 23 (2005) 738-751.
[42] D. Zhang, A.J. Paley, G. Childs, The transcriptional repressor ZFM1 interacts with and modulates the ability of EWS to activate transcription, J. Biol. Chem. 273 (1998) 18086-18091.
[43] S.L. Palmieri, W. Peter, H. Hess, H.R. Scholer, Oct-4 transcription factor is differentially expressed in the mouse embryo during establishment of the first two extraembryonic cell lineages involved in implantation, Dev. Biol. 166 (1994) 259-267.
[44] T. Barberi, L.M. Willis, N.D. Socci, L. Studer, Derivation of multipotent mesenchymal precursors from human embryonic stem cells, PLoS Med. 2 (2005) e161.
[45] H. Kimura, M. Tada, N. Nakatsuji, T. Tada, Histone code modifications on pluripotential nuclei of reprogrammed somatic cells, Mol. Cell. Biol. 24 (2004) 5710-5720.
[46] H.J. Kraft, S. Mosselman, H.A. Smits, P. Hohenstein, E. Piek, Q. Chen, K. Artzt, E.J. van Zoelen, Oct-4 regulates alternative platelet-derived growth factor alpha receptor gene promoter in human embryonal carcinoma cells, J. Biol. Chem. 271 (1996) 12873-12878.
[47] R. Kalluri, E.G. Neilson, Epithelial-mesenchymal transition and its implications for fibrosis, J. Clin. Invest. 112 (2003) 1776-1784.
[48] C. Martinez-Alvarez, M.J. Blanco, R. Perez, M.A. Rabadan, M. Aparicio, E. Resel, T. Martinez, M.A. Nieto, Snail family members and cell survival in physiological and pathological cleft palates, Dev. Biol. 265 (2004) 207-218.
[49] H. Peinado, F. Portillo, A. Cano, Transcriptional regulation of cadherins during development and carcinogenesis, Int. J. Dev. Biol. 48 (2004) 365-375.
[50] E. de Laplanche, K. Gouget, G. Cleris, F. Dragounoff, J. Demont, A. Morales, L. Bezin, C. Godinot, G. Perriere, D. Mouchiroud, H. Simonnet, Physiological oxygenation status is required for fully differentiated phenotype in kidney cortex proximal tubules, Am. J. Physiol. Renal Physiol. 291 (2006) F750-760.
[51] L.H. Looijenga, H. Stoop, H.P. de Leeuw, C.A. de Gouveia Brazao, A.J. Gillis, K.E. van Roozendaal, E.J. van Zoelen, R.F. Weber, K.P. Wolffenbuttel, H. van Dekken, F. Honecker, C. Bokemeyer, E.J. Perlman, D.T. Schneider, J. Kononen, G. Sauter, J.W. Oosterhuis, POU5F1 (OCT3/4) identifies cells with pluripotent potential in human germ cell tumors, Cancer Res. 63 (2003) 2244-2250.